nature communications

Article

https://doi.org/10.1038/s41467-025-57173-2

GRB2 regulation of essential signaling pathways in the endometrium is critical for implantation and decidualization

Received: 6 March 2024

Accepted: 12 February 2025

Published online: 04 March 2025

Check for updates

Dinh Nam Tran[1], Yeon Jeong Hwang[2], Keun Cheon Kim[1], Rong Li[1], Ryan M. Marquardt[3], Chen Chen[4], Steven L. Young[5], Bruce A. Lessey[6], Tae Hoon Kim[1], Yong-Pil Cheon[2] ✉ & Jae-Wook Jeong[1] ✉

Over 75% of failed pregnancies involve implantation defects. Growth factor receptor-bound protein 2 (GRB2) is an adaptor protein involved in signal transduction and cell communication. Here we show that the expression of GRB2 protein is lower in endometrium of infertile women with endometriosis compared to controls. Our mouse endometriosis model revealed that endometriosis development results to GRB2 loss in the eutopic endometrium. To understand the role of GRB2 in the uterus, we generated mice with conditional ablation of *Grb2* in the *Pgr* positive cells (*Grb2*$^{d/d}$). *Grb2*$^{d/d}$ mice were infertile due to implantation failure. Although ovarian functions were normal, *Grb2*$^{d/d}$ mice had a non-receptive endometrium due to progesterone resistance and dysregulation of steroid hormone and FOXA2 signaling pathways. Furthermore, our results were supported by findings of GRB2 attenuation in primary human endometrial stromal cells from women with endometriosis. Our results demonstrate that GRB2 is critical for endometrial receptivity and decidualization.

Six percent of women under 44 are infertile, 12% have difficulty getting pregnant or carrying pregnancies to term, and over 75% of failed pregnancies involve implantation defects[1]. Even the most successful treatments, such as assisted reproductive technologies, still lead to frequent implantation failures. Uterine receptivity, implantation, and decidualization are critical in supporting embryonic growth. These events are regulated by the coordinated actions of estrogen (E2) and progesterone (P4) that are produced and secreted by the ovary. E2 stimulates uterine epithelial cell proliferation, and P4 suppresses E2-induced proliferation. E2 and P4 act on the endometrium and myometrium directly through their cognate nuclear receptors, the progesterone receptor (PGR) and estrogen receptors (ESR1 and ESR2), respectively, and indirectly by stimulation of various growth factors including EGF. During implantation, changes in the expression of adhesion molecules, cytokines, and transcriptional factors are dependent upon E2 and P4. Because of the complexity and dynamic nature of implantation, these molecular changes are still not fully understood.

In rodents, E2 promotes proliferation of epithelial cells in the endometrium to initiate the preparation for pregnancy on gestation day 0.5 (GD 0.5). Subsequently, P4 inhibits E2-induced proliferation of uterine epithelial cells and stimulates stromal cell proliferation on GD 3.5[2,3]. Rapid induction of the cytokine leukemia-inhibitory factor (LIF) by nidatory estrogen with elevated P4 levels is a critical step for uterine receptivity[4–6]. The blastocyst attaches to the uminal epithelium on GD 4.5, and implantation occurs followed by decidualization of the

[1]Department of Obstetrics, Gynecology and Women's Health, University of Missouri School of Medicine, Columbia, MO, USA. [2]Division of Developmental Biology and Physiology, Department of Biotechnology, Institute of Basic Sciences, Sungshin Women's University, Seoul, South Korea. [3]Department of Obstetrics, Gynecology & Reproductive Biology, Michigan State University, Grand Rapids, MI, USA. [4]Department of Animal Science, Michigan State University, East Lansing, MI, USA. [5]Department of Obstetrics, Gynecology and Women's Health, Duke University, Durham, NC, USA. [6]Department of Obstetrics and Gynecology, Wake Forest Baptist Health, Winston-Salem, NC, USA. ✉e-mail: ypcheon@sungshin.ac.kr; jeongjw@missouri.edu

surrounding stroma[2,7]. During decidualization, uterine stromal cells undergo proliferation and differentiation into large epithelioid decidual cells, which creates a local environment permissive to implantation and supportive of the embryo. Similar to the mouse, the steroid hormones E2 and P4 are critical for the regulation of human endometrium including proliferation, secretion, and menstrual shedding. Defective stromal cell decidualization can result in pregnancy complications including pregnancy loss and miscarriage in mice and human[2].

Uterine glands and their secretory products are likely critical regulators of blastocyst implantation, uterine receptivity, and conceptus growth and development in both mice and humans[8]. During pregnancy, uterine glands present in the endometrium surrounding the embryo implantation site and develop decidua[9,10]. Defective development of uterine glands can be causing pregnancy loss[10]. Forkhead box a2 (FOXA2), a member of FoxA family transcription factors, has important roles in the uterine function and implantation[11]. *Foxa2* is only found expressed in the glandular epithelium of the uterus[12] and loss of expression defects endometrial gland development resulting in the loss of uterine glands[11]. Therefore, FOXA2-deficient mice lack of *Lif* secretion and thus are infertile[11,13]; however, the upstream regulators of FOXA2 are not completely understood in relation to their uterine functions.

Growth factor receptor-bound protein 2 (GRB2) is an adapter protein critical for the regulation of cell survival, proliferation, differentiation, and metabolism[14]. GRB2 directly binds EGFR and activates ERK1/2 and AKT in a Ras-dependent manner[15]. Abnormal expression of GRB2 promotes tumor malignancies by activating both PI3K/AKT and EGFR/ERK pathways[16,17]. In contrast, downregulation of GRB2 protein expression induced cell growth inhibition[18]. EGFR and ERK1/2 critically regulate endometrial function during early pregnancy[19,20]. EGFR plays important roles in epithelial cell proliferation/differentiation and stromal cell decidualization during early pregnancy. However, the role of GRB2 in implantation and decidualization has not been studied.

Here, we show that the amount of GRB2 is decreased in endometrium from infertile women with endometriosis. We used uterine-specific *Grb2* knock-out mice and primary human endometrial stromal cells to demonstrate that GRB2 is necessary for implantation and decidualization. Our uterine-specific *Grb2* knock-out mice display a non-receptive endometrium due to dysregulation of ovarian steroid hormone signaling as well as FOXA2 signaling.

Results

The levels of GRB2 protein are diminished in endometrium from infertile women with endometriosis

We examined the levels of GRB2 proteins in endometrium from fertile women (n = 19) and infertile women with and without endometriosis (n = 18 and n = 13, respectively) using immunohistochemistry (Fig. 1a). Our immunohistochemistry result revealed strong expression of GRB2 in the endometrial epithelial and stromal cells from control group endometrium at secretory stage. However, the expression of GRB2 proteins was significantly decreased in the epithelial cells ($p < 0.001$ and $p < 0.01$, respectively) and stromal cells ($p < 0.001$ and $p < 0.01$, respectively) of the eutopic endometrium from infertile women without and with endometriosis compared to controls (Fig. 1a). These results suggest that GRB2 deficiency may be associated with female infertility. To investigate the effect of *Grb2* loss in endometriosis and pregnancy, we generated a mouse model with *Grb2* conditionally ablated in *Pgr*-positive cells ($Pgr^{cre/+}Grb2^{f/f}$; $Grb2^{d/d}$). Ablation of *Grb2* in the uterus was confirmed by Western blot and immunohistochemical analyses (Fig. 1b, c). Our Western blot result showed a remarkable decrease of GRB2 protein in the whole uteri of $Grb2^{d/d}$ mice compared to control ($Grb2^{f/f}$) mice (Fig. 1b). Immunohistochemical analysis validated that GRB2-postivite cells were undetectable in the uterine epithelial and stromal cells of female $Grb2^{d/d}$ at GD 3.5 (Fig. 1c).

To determine whether *Grb2* deficient endometrial tissues exhibit different behavior when transplanted into an endometriosis model in mice, we performed endometriosis induction with normal GRB2-positive endometrium ($Pgr^{cre/+}Rosa26^{mTmG/+}$ control) and endometrium that lacks GRB2 ($Pgr^{cre/+}Grb2^{f/f}$ $Rosa26^{mTmG/+}$; $Grb2^{d/d}$ $Rosa26^{mTmG/+}$). While GFP-positive endometriotic lesions were detected in mice with normal GRB2-positive endometrium, we could not detect any endometriotic lesions in mice with *Grb2* deficient endometrial tissues (Fig. 1d). We also determine whether GRB2 expression is attenuated after endometriosis development. GRB2 was significantly lower in epithelial ($p < 0.05$ and $p < 0.05$, respectively) as well as stromal cells ($p < 0.05$ and $p < 0.001$, respectively) of the eutopic endometrium from mice with endometriosis compared to the sham control group at 1 month and 3 months after endometriosis induction (Fig. 1e). Thus, our results suggest that endometriosis development and progression are associated with a loss of GRB2 in the eutopic endometrium that may result in infertility.

Grb2 loss results in female infertility

We examined the expression of GRB2 to determine the cell-specific and temporal expression profiles of GRB2 in uteri of pregnant wild-type female mice from GD 0.5 to 7.5 using immunohistochemistry analysis. Our immunohistochemistry showed dynamic expressions of GRB2 proteins during early pregnancy (Fig. 2a). GRB2 proteins were weakly detected in uterine stromal cells of wild-type mice at GD 0.5. The levels of GRB2 proteins gradually increased from GD 2.5 to GD 3.5. At implantation stage GD 4.5, we detected strong GRB2 expression in decidual cells surrounding implantation sites. At GD 5.5, stromal cells underlying the implantation chamber differentiate into epithelioid cells to form the primary decidual zone (PDZ)[21]. GRB2-positive cells were detected in the PDZ at GD 5.5, but the intensity was decreased in the PDZ at GD 7.5. In contrast to the dynamic changes in the stroma, GRB2 expression was consistently strong in luminal and glandular epithelial cells from GD 0.5 to GD 4.5. These results suggest that GRB2 may play an important role during early pregnancy.

To explore the functional role of uterine *Grb2* in pregnancy, we performed a fertility test where female $Grb2^{f/f}$ and $Grb2^{d/d}$ mice were mated with wild-type male mice, and their litters and pups were examined for 6 months (n = 5). $Grb2^{f/f}$ control mice gave birth to an average of 4.37 ± 0.24 litter per mouse and an average of 6.19 ± 0.28 pups per litter, whereas all $Grb2^{d/d}$ mice were sterile (Table 1). The results of the fertility test suggest that *Grb2* plays an important role in pregnancy.

Because of reported Cre recombinase expression within the pituitary, ovary, uterus, and mammary gland of the $Pgr^{cre/+}$ mouse[22], we reasoned that $Grb2^{d/d}$ infertility might result from ovarian defects. To determine whether $Grb2^{d/d}$ mice had any ovarian phenotypes, we examined levels of serum E2 and P4 as well as ovarian histology (n = 5). The serum level of E2 and P4 showed no significant difference between $Grb2^{f/f}$ (E2 = 7.87 ± 0.94 pg/ml and P4 = 8.01 ± 1.20 ng/ml) and $Grb2^{d/d}$ (E2 = 6.85 ± 0.95 pg/ml and P4 = 6.48 ± 1.01 ng/ml) mice at GD 3.5 (Supplementary Fig. 1a). $Grb2^{d/d}$ mice showed normal ovarian morphology comparable to $Grb2^{f/f}$ mice (Supplementary Fig. 1b). These results suggest that $Grb2^{d/d}$ female mice have normal ovarian functions and that the infertility of $Grb2^{d/d}$ female mice results from uterine dysfunction.

$Grb2^{d/d}$ female mice fail to support pregnancy past implantation

To determine the cause of infertility in $Grb2^{d/d}$ mice, ultrasound imaging was used to monitor pregnancy in $Grb2^{f/f}$ and $Grb2^{d/d}$ mice during early pregnancy. The embryos were detected in $Grb2^{f/f}$ but not $Grb2^{d/d}$ mice at GD 5.5, 7.5, and 9.5 by ultrasonography (Supplementary Fig. 2a), and the 3D reconstructions were generated to reveal the shape and size of implantation sites (Supplementary Fig. 2b). The sizes of embryos in $Grb2^{f/f}$ mice gradually increased during early pregnancy,

https://doi.org/10.1038/s41467-025-57173-2

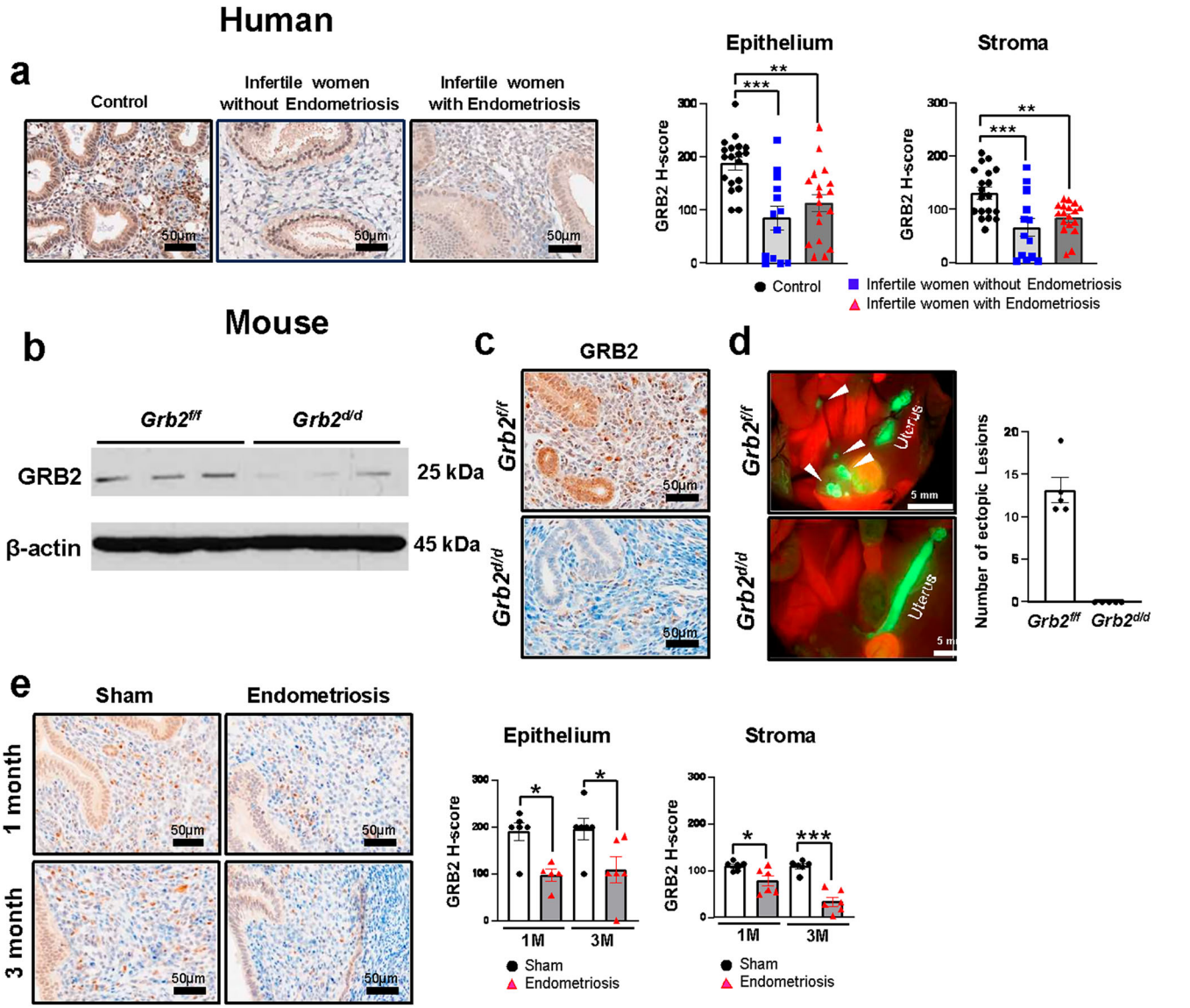

Fig. 1 | The expression of GRB2 was decreased in the endometrium of women with endometriosis and women without endometriosis. a Representative image of GRB2 immunohistochemistry in the endometrium from infertile women with endometriosis ($n = 18$), infertile women without endometriosis ($n = 13$) compared to controls ($n = 19$) at mild-secretory stage. The quantification of GRB2 immunohistochemistry in the stroma and epithelial cells of endometrium from women with endometriosis, women without endometriosis and control. The results represent the mean ± SEM. $^{***}p = 0.0002$, $^{**}p = 0.0033$, $^{***}p = 0.0007$, $^{**}p = 0.0086$ by Ordinary one-way ANOVA test. **b**, **c** The ablation of GRB2 in the uterus were confirmed by Western blot analysis (n = 3 per genotype) and immunohistochemistry in the uteri of *Grb2*$^{f/f}$ and *Grb2*$^{d/d}$ mice at GD 3.5 (n = 5 per genotype). **d** Representative fluorescence photomicrographs and average total number of endometriotic sites in *Grb2*$^{f/f}$ and *Grb2*$^{d/d}$ mice by induced endometriosis based on *mT/mG* mice (n = 5 per genotype). Endometriotic lesions were visualized by GFP expression in the outside of uterus. White arrow indicates endometriotic lesions. The results represent the mean ± SEM by two-tailed unpaired t-test. **e** Immunohistochemistry GRB2 analysis from uteri of the endometrium from 1 month and 3 months after endometriosis induction and Sham mice at GD 3.5 (n = 6 per genotype and time point). Semi-quantitative analysis of GRB2 levels in the epithelium and stroma in the stroma and epithelial cells endometrium from 3 months after endometriosis induction and Sham mice at GD 3.5. The results represent the mean ± SEM. $^{*}p = 0.0334$, $^{*}p = 0.0234$ and $^{*}p = 0.0384$, $^{*}p = 0.0445$, $^{***}p < 0.0001$ by Ordinary one-way ANOVA test. Source data are provided in the Source Data file.

the average sizes being 2.19 ± 0.34 mm^3 at GD 5.5, 6.86 ± 0.83 mm^3 at GD 7.5 and 24.87 ± 1.3 mm^3 at GD 9.5 (Supplementary Fig. 2c). However, we could not detect any embryos in *Grb2*$^{d/d}$ mice at GD 5.5, GD 7.5, or GD 9.5 (Supplementary Fig. 2d). Our results suggest that *Grb2*$^{d/d}$ mice were infertile due to early pregnancy loss.

Grb2$^{d/d}$ mice exhibit implantation defects

In order to determine the cause of early pregnancy loss in *Grb2*$^{d/d}$ mice, female *Grb2*$^{f/f}$ and *Grb2*$^{d/d}$ mice were examined at implantation stage GD 4.5. Implantation sites were visualized by intravenous injection of Chicago blue (Fig. 2b; n = 6). Although *Grb2*$^{f/f}$ mice revealed normal 8.29 ± 0.49 implantation sites, *Grb2*$^{d/d}$ mice did not show any Chicago blue-stained implantation sites (Fig. 2b). Next, our histological analysis revealed that embryos in *Grb2*$^{f/f}$ mice were attached to the luminal epithelium and surrounded by decidualized cells in (Fig. 2c). However, H&E staining for *Grb2*$^{d/d}$ mice revealed two groups of implantation sites in the uteri of (Fig. 2c). In group #1 (n = 3), the uterine lumen was not closed, and the embryos were free-floating within the uterine lumen. (Fig. 2c). In group #2 (n = 3), the uterine lumen was closed; however, the blastocysts were loosely affixed to the luminal epithelium and decidual cells were not observed (Fig. 2c). We performed IHC for prostaglandin-endoperoxide synthase 2 (PTGS2; COX2), a decidualization marker[23],

https://doi.org/10.1038/s41467-025-57173-2

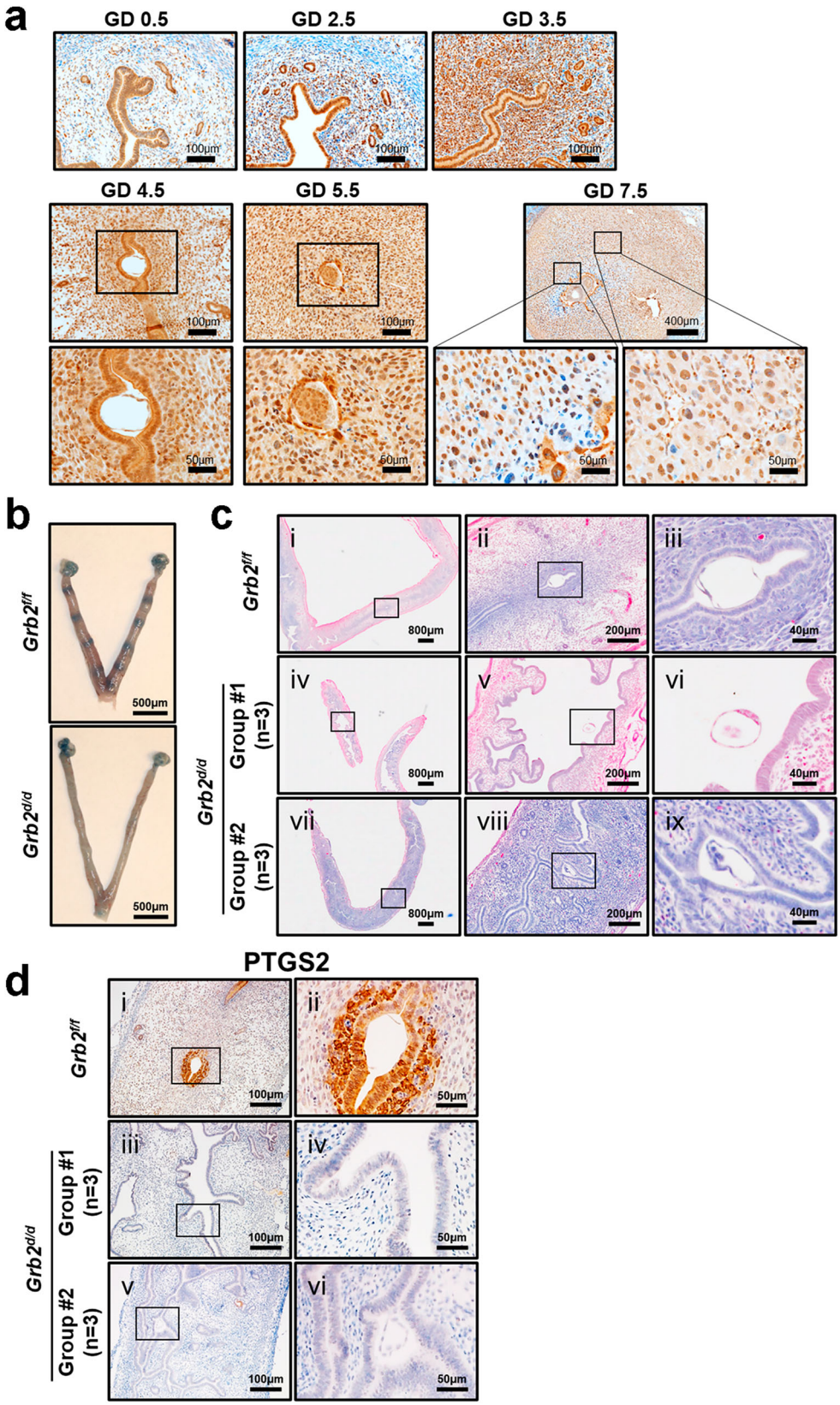

Fig. 2 | Implantation defect and altered PTGS2 expression in *Grb2*$^{d/d}$ mice at GD 4.5. a Representative image of GRB2 immunohistochemistry in the uterine tissue from GD 0.5 to GD 7.5 (n = 5 per time point). **b** Visualizations of implantation sites by Chicago Sky Blue 6B dye in *Grb2*$^{f/f}$ and *Grb2*$^{d/d}$ uteri at GD 4.5 (n = 6 per genotype) after intravenous injection of Chicago Sky Blue 6B dye. **c** Hematoxylin and eosin analysis of implantation sites from uteri of *Grb2*$^{f/f}$ (i–iii) and *Grb2*$^{d/d}$ (iv–ix) mice at GD 4.5. **d** Immunohistochemistry PTGS2 analysis from uteri of *Grb2*$^{f/f}$ (i and ii) and *Grb2*$^{d/d}$ (iii–vi) mice at GD 4.5 (n = 3).

https://doi.org/10.1038/s41467-025-57173-2

Table 1 | Fertility test of *Grb2*$^{d/d}$ mice

	Number of mice tested	Number of litters	Number of pups	Average of pups/litter	Average number of litter/mouse
Grb2$^{f/f}$	5	27	167	6.19 ± 0.28	4.37 ± 0.24
Grb2$^{d/d}$	5	0	0	0	0

Grb2$^{f/f}$ mice produced a normal number of litters and pups/litter over a 6-month period of mating, but *Grb2*$^{d/d}$ mice were infertile (n = 5).

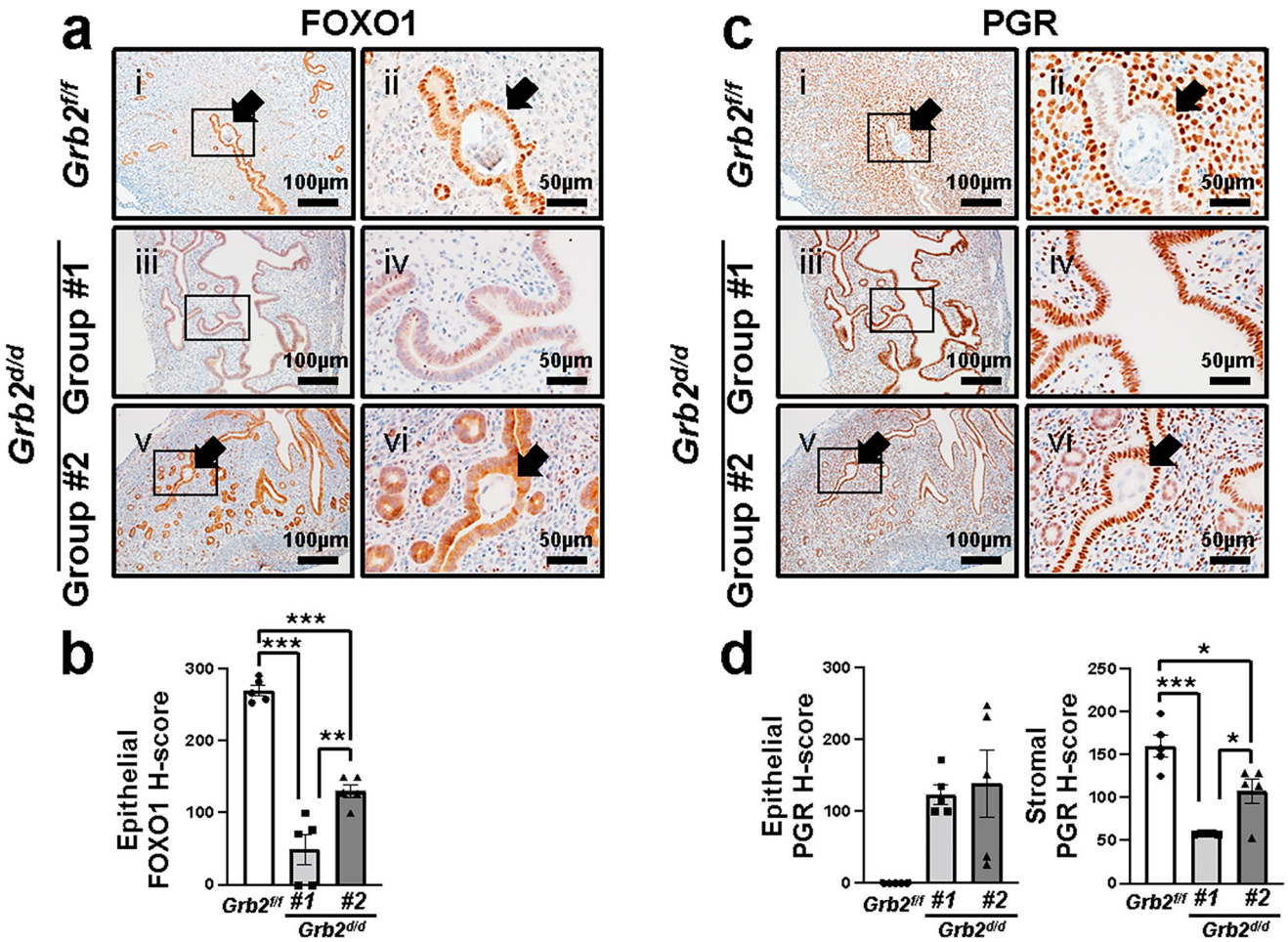

Fig. 3 | Dysregulation of FOXO1 and PGR at the implantation sites of *Grb2*$^{d/d}$ mice at GD 4.5. a Immunohistochemistry analysis of FOXO1 from the uteri of *Grb2*$^{f/f}$ (i and ii) and *Grb2*$^{d/d}$ (iii–vi) mice at GD 4.5. **b** Semi-quantitative analysis of FOXO1 levels in the epithelium of *Grb2*$^{f/f}$ and *Grb2*$^{d/d}$ mice at GD 4.5 (n = 5 per group). The results represent the mean ± SEM. ***$p < 0.0001$, ***$p < 0.0001$, and **$p = 0.0033$ by Ordinary one-way ANOVA test. **c** Immunohistochemistry analysis of PGR from the uteri of *Grb2*$^{f/f}$ (i and ii) and *Grb2*$^{d/d}$ (iii–vi) mice at GD 4.5. **d** Semi-quantitative analysis of PGR levels in the epithelium and stroma of *Grb2*$^{f/f}$ and *Grb2*$^{d/d}$ mice at GD 4.5 (n = 5 per group). The results represent the mean ± SEM. ***$p < 0.0001$, *$p = 0.0125$, and *$p = 0.0163$ by Ordinary one-way ANOVA test. Source data are provided in the Source Data file.

to examine decidualization at implantation sites. *Grb2*$^{f/f}$ mice showed strong PTGS2 staining in the decidual cells surrounding the embryos (Fig. 2d). However, we could not observe any PTGS2 expression in luminal epithelium and implantation sites in Group #1 or #2 of *Grb2*$^{d/d}$ mice (Fig. 2d). These results show *Grb2*$^{d/d}$ mice were infertile due to defective embryo implantation and decidualization.

Grb2$^{d/d}$ mice exhibit dysregulation of PGR/FOXO1 and EGFR/ERK signaling in implantation

PGR and FOXO1 are important transcription factors regulating epithelial integrity and decidualization during implantation, and they are expressed reciprocally to each other[24,25]. We assessed the expression of FOXO1 and PGR in the implantation sites of *Grb2*$^{f/f}$ and *Grb2*$^{d/d}$ mice at GD 4.5 (Fig. 3; n = 5). FOXO1 proteins were strongly expressed in the nuclei of luminal epithelial cells in *Grb2*$^{f/f}$ mice (Fig. 3a, b). However, the expression of FOXO1 was significantly decreased ($p < 0.001$ and $p < 0.001$, respectively) in both Group #1 and Group #2 of *Grb2*$^{d/d}$ mice compared to control (Fig. 3a, b). Importantly, the localizations of FOXO1 were mainly in cytoplasm instead of nuclear. Moreover, its expression in Group #1 was significantly 2.6 times lower ($p < 0.01$) than in Group#2 (Fig. 3b). The nuclear expression of FOXO1 proteins at implantation sites of controls coincides with PGR loss in luminal epithelium and strong expression of PGR in stroma (Fig. 3c, d). However, the levels of nuclear PGR in luminal epithelium were highly increased in both Group #1 and Group #2 of *Grb2*$^{d/d}$ mice compared to controls (Fig. 3d). In contrast to luminal epithelium, stromal PGR protein was significantly decreased in both Group #1 and Group #2 of *Grb2*$^{d/d}$ mice compared to control mice (Fig. 3d; $p < 0.001$ and $p < 0.05$, respectively). Moreover, its expression in Group #2 was significantly higher ($p < 0.05$) than in Group#1 (Fig. 3d). Our IHC results suggest that the dysregulation of PGR and FOXO1 at implantation sites causes implantation failure of *Grb2*$^{d/d}$ mice.

Grb2$^{d/d}$ mice exhibit decidualization defects

Decidualization is a process of stromal differentiation during embryo implantation[26]. However, it is difficult to examine the effect of GRB2 loss on decidualization during early pregnancy because *Grb2*$^{d/d}$ mice have implantation failure. To investigate the role of *Grb2* in decidualization, we applied a mouse artificial decidualization model in *Grb2*$^{d/d}$ mice. Ovariectomized female *Grb2*$^{f/f}$ and *Grb2*$^{d/d}$ mice were hormonally and physically stimulated to artificially induce decidualization, mimicking an invading embryo in the left horn of the uterus. The other uterine horn was left unstimulated as a control. Although *Grb2*$^{f/f}$ mice displayed a decidual uterine horn that responded well to this artificial induction, *Grb2*$^{d/d}$ mice displayed a defect of decidual response (Fig. 4a). The weight ratio of stimulated to control horn was significantly decreased ($p < 0.001$) in *Grb2*$^{d/d}$ mice (1.06 ± 0.07, $n = 4$) compared to *Grb2*$^{f/f}$ mice (16.42 ± 1.74, $n = 5$) (Fig. 4a). Histological analysis confirmed that the stimulated uterine horn from control mice showed enlarged, cuboidal decidual cells, but the *Grb2*$^{d/d}$ mice did not detect decidual cells in the stimulated uterine horns (Fig. 4b). Further, the expression of the known decidualization markers, bone morphogenetic protein 2 (*Bmp2*) ($p < 0.001$), follistatin (*Fst*) ($p < 0.001$), FK506-binding protein 5 (*Fkbp5*) ($p < 0.01$), and wingless-related mouse mammary tumor virus integration site 4 (*Wnt4*) ($p < 0.01$), were significantly decreased in the decidual uterine horn of *Grb2*$^{d/d}$ mice compared to the decidual uterine horn of *Grb2*$^{f/f}$ ($n = 4$) (Fig. 4c).

Infertile women with endometriosis display markedly reduced decidualization and impaired uterine receptivity[27]. Therefore, we examined GRB2 levels in primary human endometrial stromal cells (hESCs) from women with or without endometriosis using RT-qPCR. GRB2 levels were significantly lower ($p < 0.001$) in hESCs from women with endometriosis compared to controls (Fig. 4d). hESCs can be cultured in vitro and treated with a hormone cocktail of E2, P4, and cAMP (EPC) to induce decidualization[28]. To determine the effect of GRB2 attenuation on human decidualization, we combined this system with a siRNA loss of function approach in control hESCs. The *GRB2* knockdown efficiency was assessed by RT-qPCR before inducing decidualization, confirming that *GRB2* mRNA levels were significantly decreased in hESCs treated with *GRB2* siRNA compared with non-targeting pool siRNA (Fig. 4d). hESC transfected with a non-targeting pool of control siRNA and treated with EPC showed robust induction of classic decidual markers *IGFBP1* and *PRL* (Fig. 4d). Conversely, in cells transfected with *GRB2* siRNA, the induction of these markers was significantly reduced compared to the control (Fig. 4d). These results indicated that GRB2 plays an important role for decidualization in mice as well as hESCs.

Mice with *Grb2* conditional deletion in the uterine epithelium showed normal fertility

Uterine epithelial-stromal crosstalk is crucial for implantation and decidualization[7]. GRB2 proteins are strongly expressed in uterine epithelial and stromal cells at pre-implantation stage. To examine the role of *Grb2* in uterine epithelium, we conditionally ablate *Grb2* in the adult mouse endometrial endometrium by crossing *Ltf*$^{icre/+}$[29] and *Grb2*$^{f/f}$ mice. *Ltf*$^{icre/+}$*Grb2*$^{f/f}$ mice displayed *Grb2* deletion in the luminal and glandular epithelium, while retaining *Grb2* expression in the stroma in contrast to *Grb2*$^{d/d}$ mice (Supplementary Fig. 3a). To assess overall fecundity, control *Grb2*$^{f/f}$ and *Ltf*$^{icre/+}$*Grb2*$^{f/f}$ females were mated with wild-type male mice ($n = 5$). *Grb2*$^{f/f}$ and *Ltf*$^{icre+}$*Grb2*$^{f/f}$ mice had normal number of pups with an average of 5.89 ± 0.078 and 5.71 ± 0.079 pups per litter, respectively (Supplementary Fig. 3b). *Ltf*$^{icre+}$*Grb2*$^{f/f}$ mice revealed normal ovarian functions including ovulation, fertilization and histology (Supplementary Fig. 3c, d). We also monitored pregnancy and embryo growth in *Ltf*$^{icre+}$*Grb2*$^{f/f}$ mice using high frequency ultrasound. Normal sizes and numbers of embryos were detected at GD 5.5, GD 7.5, and GD 9.5 in both *Grb2*$^{f/f}$ and *Ltf*$^{icre+}$*Grb2*$^{f/f}$ mice (Supplementary Fig. 4a). Furthermore, the number of implantation sites were no different between *Ltf*$^{icre+}$*Grb2*$^{f/f}$ and *Grb2*$^{f/f}$ mice using Chicago blue at GD 4.5, GD 5.5 and GD 9.5 mice (Supplementary Fig. 4b). In addition, both *Grb2*$^{f/f}$ and *Ltf*$^{icre+}$*Grb2*$^{f/f}$ mice revealed normal decidual responses by artificial decidualization experiment (Supplementary Fig. 4c). These results demonstrated that epithelial *Grb2* ablation does not impair implantation and decidualization.

Grb2 loss results in a non-receptive endometrium due to dysregulation of ovarian steroid hormone signaling

Loss of epithelial E2 action is essential for implantation at the secretory phase in all eutherian mammal species studied[30–32]. Proliferation is markedly reduced in epithelial cells at the peri-implantation stage for embryo attachment[20,33]. We examined expression of Ki67, a proliferation marker, at GD 3.5, which marks the pre-implantation stage[2] (Fig. 5a). While cell proliferation in the luminal epithelium was significantly increased ($p < 0.001$) in *Grb2*$^{d/d}$ mice (95.21 ± 1.91 %) compared to control *Grb2*$^{f/f}$ mice (3.99 ± 1.58 %), cell proliferation in the stroma was significantly decreased ($p < 0.001$) in *Grb2*$^{d/d}$ mice (7.49 ± 3.04 %) compared with *Grb2*$^{f/f}$ mice (63.77 ± 4.59 %). Next, we investigated whether *Grb2* ablation caused excess E2 signaling. The expression of *Clca3*, *Ltf*, and *Muc-1*, E2 target genes, were significantly increased ($p < 0.01$, $p < 0.05$, and $p < 0.001$, respectively) in *Grb2*$^{d/d}$ mice compared to control mice (Fig. 5b). We also detected a significant decrease ($p < 0.01$) of ESR1 levels in stromal cells of *Grb2*$^{d/d}$ mice compared to control *Grb2*$^{f/f}$ mice but not in epithelial cells (Fig. 5c). These results demonstrate that E2 activity is enhanced in uterine epithelial cells of the *Grb2*$^{d/d}$ mice.

Defective P4 action is the primary cause of the defects in ESR1 downregulation, and has been called P4 resistance[34]. Next, we used RT-qPCR and immunohistochemistry to assess expression of P4 target genes and PGR in *Grb2*$^{d/d}$ mice. mRNA levels of P4 target genes *Il13ra2*, *Fst*, *Areg*, and *Lrp2* were significantly downregulated ($p < 0.01$, $p < 0.001$, $p < 0.01$, and $p < 0.001$, respectively) in *Grb2*$^{d/d}$ mice compared to control mice (Fig. 5d). Interestingly, stromal PGR expression was significantly reduced ($p < 0.001$) in *Grb2*$^{d/d}$ mice compared to control mice (Fig. 5e). However, the expression of epithelial PGR did not change in *Grb2*$^{d/d}$ mice (Fig. 5e). Moreover, expression of the stromal markers, vimentin and COUP-TFII, was significantly decreased ($p < 0.001$ and $p < 0.001$, respectively) in the stromal cells of *Grb2*$^{d/d}$ mice compared to control mice (Fig. 5f, g). These results suggest that GRB2 loss results in a non-receptive endometrium due to dysregulation of ovarian steroid hormone signaling.

Grb2 regulates the E2/P4-related as well as EGF-related genes

To identify the signaling pathways that *Grb2* regulates at pre-implantation, we performed RNA-seq analysis in the uterine tissue of *Grb2*$^{f/f}$ and *Grb2*$^{d/d}$ mice at GD 3.5. Our transcriptomic analysis identified 2243 differentially expressed genes (DEGs) (fold change > 2, $p < 0.05$ and FDR < 0.05) including 917 upregulated genes and 1326 down-regulated genes in the uterus of *Grb2*$^{d/d}$ mice compared with *Grb2*$^{f/f}$ mice (Supplementary Data 1). Upstream regulator analysis by Ingenuity Pathway Analysis (IPA) showed that major altered pathways in the *Grb2*$^{d/d}$ uterus included 17β-estradiol/ESR1, progesterone/PGR, STAT3, FOXO1, and EGF/EGFR signaling (Fig. 6a). Our pathway analysis by IPA identified 508 differentially expressed E2-related genes (Supplementary Data 2) and 191 differentially expressed P4-related (Supplementary Data 3) genes in *Grb2*$^{d/d}$ uteri compared with *Grb2*$^{f/f}$ uteri (Fig. 6b). Importantly, 246 EGF/EGFR-related genes were identified in *Grb2*$^{d/d}$ mice compared with *Grb2*$^{f/f}$ mice (Fig. 6c and Supplementary Data 4). Because EGFR critically regulates endometrial function and decidualization during early pregnancy[19], and GRB2 interacts with EGFR to activate Ras and its downstream kinases, ERK1/2[14], we validated our transcriptomic results using RT-qPCR. Our RT-qPCR results revealed that the mRNA

https://doi.org/10.1038/s41467-025-57173-2

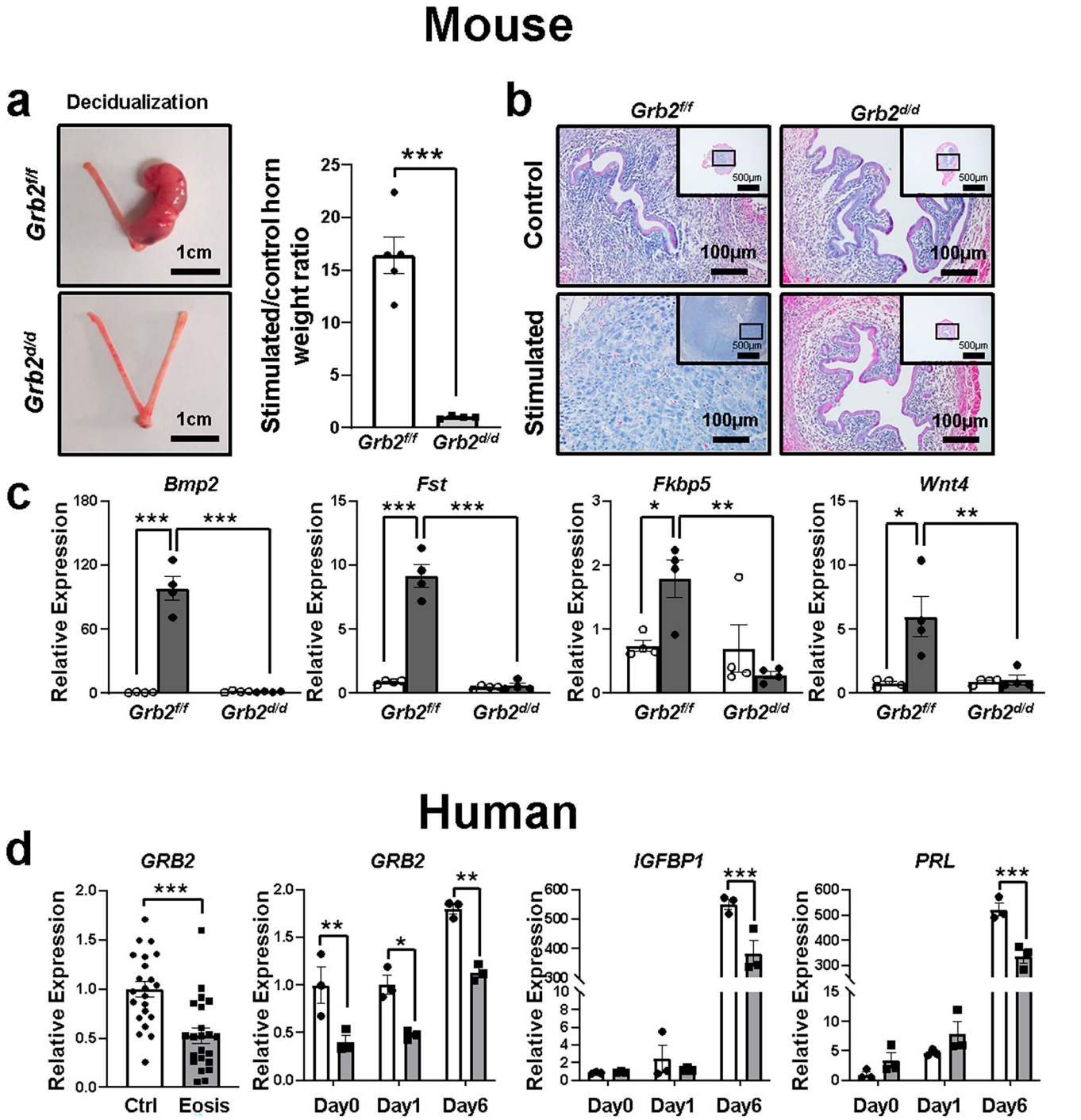

Fig. 4 | Decidualization defects in *Grb2*$^{d/d}$ mice and hESCs. a A decrease of the stimulated/control uterine weight ratio in *Grb2*$^{f/f}$ and *Grb2*$^{d/d}$ mice at decidualization day 5 (n = 5 for *Grb2*$^{f/f}$ and n = 4 for *Grb2*$^{d/d}$ mice). The results represent the mean ± SEM. ***$p = 0.0001$ by two-tailed unpaired t-test. **b** Hematoxylin and eosin (H&E) staining in control and stimulated horn of *Grb2*$^{f/f}$ and *Grb2*$^{d/d}$ mice at decidualization day 5. **c** RT-qPCR analysis for the expression of decidualization marker genes, *Bmp2*, *Fst*, *Fkbp5*, and *Wnt4*, in the uteri of *Grb2*$^{f/f}$ and *Grb2*$^{d/d}$ mice (n = 4 per genotype). The results represent the mean ± SEM. ***$p < 0.0001$, ***$p < 0.0001$, ***$p < 0.0001$, ***$p < 0.0001$, *$p = 0.0435$, **$p = 0.0045$, **$p = 0.0034$, **$p = 0.0042$ by Ordinary one-way ANOVA test. **d** The expression of *GRB2* in hESCs from control women without (Ctrl) and with (Eosis) endometriosis (n = 22 per group). The expression of *GRB2*, *IGFBP1*, and *PRL* levels in hESCs and after silencing with siRNA in decidualized HESCs. Each treatment was performed with at three biological replicates (n = 3 per group and time point). The results represent the mean ± SEM. ***$p = 0.0001$, **$p = 0.0085$, *$p = 0.0200$, **$p = 0.0035$, ***$p = 0.0004$, and ***$p < 0.0001$, by Ordinary one-way ANOVA test. Source data are provided in the Source Data file.

expression of *Egfr* was significantly ($p < 0.05$) decreased (−1.78-fold) in the *Grb2*$^{d/d}$ mice compared to the *Grb2*$^{f/f}$ mice (Fig. 6d). The levels of *Erbb2* and *Erbb3* mRNA were significantly ($p < 0.05$ and $p < 0.001$, respectively) increased (2.38-fold and 2.98-fold) in the *Grb2*$^{d/d}$ mice compared to the *Grb2*$^{f/f}$ mice, respectively. In addition, the expression of *Egf* mRNA was no different between *Grb2*$^{d/d}$ (1.82 ± 0.26) and *Grb2*$^{f/f}$ mice (1.51 ± 0.28) (Supplementary Fig. 5). The expression of ERBB2 protein was not different in the uterus of both *Grb2*$^{f/f}$ and *Grb2*$^{d/d}$ mice (Supplementary Fig. 5) but EGFR protein level was remarkably decreased in the epithelial and stromal cells of *Grb2*$^{d/d}$ mice (Fig. 6d).

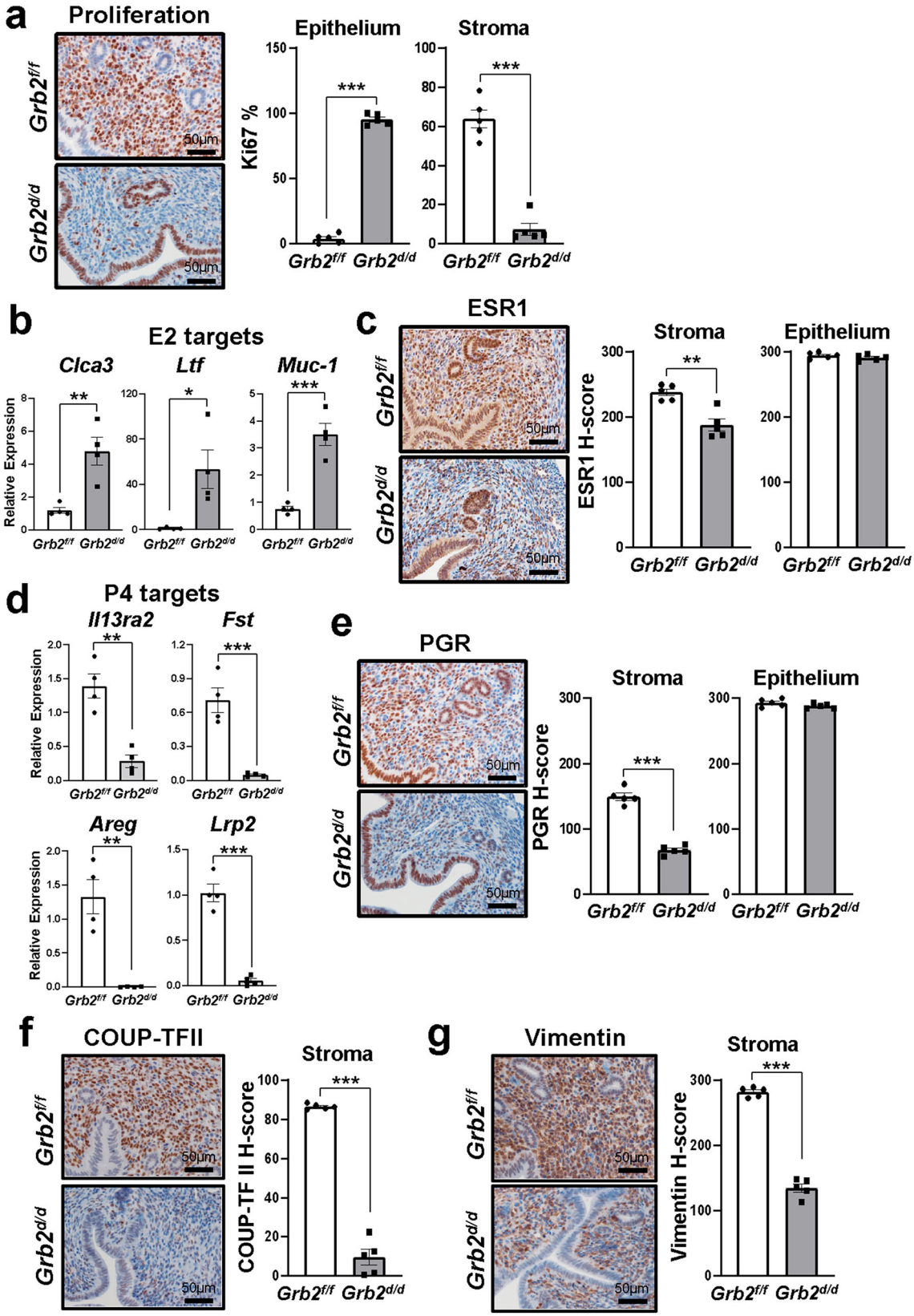

Mice lacking *Egfr* in the uterus failed to maintain and process decidualization during implantation[19]. Therefore, we next examined the expression of EGFR proteins at implantation sites of $Grb2^{f/f}$ and $Grb2^{d/d}$ mice at GD 4.5 (Fig. 6e, f). While EGFR proteins were strongly expressed at stromal cells near implantation sites of $Grb2^{f/f}$ mice, it was not detected at luminal epithelium. The levels of stromal EGFR proteins were significantly ($p < 0.001$ and $p < 0.001$, respectively) reduced in both Group #1 and Group #2 of $Grb2^{d/d}$ mice compared to control (Fig. 6f). However, the levels of epithelial EGFR proteins were significantly ($p < 0.05$ and $p < 0.05$, respectively) increased in both Group #1 and Group #2 of $Grb2^{d/d}$ mice compared to control. Furthermore, pERK1/2 proteins were strongly expressed in stromal cells

Fig. 5 | Loss of *Grb2* in uterine results in non-receptive endometrium due to progesterone resistance. a Immunohistochemistry of Ki67 analysis in the uteri of $Grb2^{f/f}$ and $Grb2^{d/d}$ mice at GD 3.5 (n = 5 per genotype). The results represent the mean ± SEM. ***$p < 0.0001$ and ***$p < 0.0001$ by two-tailed unpaired t-test. **b** RT-qPCR analysis for E2 target genes, *Clca3*, *Ltf*, and *Muc-1*, in the uteri of $Grb2^{f/f}$ and $Grb2^{d/d}$ mice at GD 3.5 (n = 4 per genotype). The results represent the mean ± SEM. **$p = 0.0063$, *$p = 0.0221$, and ***$p = 0.0006$ by two-tailed unpaired t-test. **c** Immunohistochemistry of ESR1 analysis in the uteri of $Grb2^{f/f}$ and $Grb2^{d/d}$ mice at GD 3.5 (n = 5 per genotype). The results represent the mean ± SEM. **$p = 0.0014$ by two-tailed unpaired t-test. **d** RT-qPCR analysis for P4 target genes, *Il13ra2*, *Fst*, *Areg*, and *Lrp2*, in the uteri of $Grb2^{f/f}$ and $Grb2^{d/d}$ mice at GD 3.5 (n = 4 per genotype). The results represent the mean ± SEM. **$p = 0.0015$, ***$p = 0.0009$, **$p = 0.0019$ and ***$p < 0.0001$ by two-tailed unpaired t-test. **e** Immunohistochemistry of PGR analysis in the uteri of $Grb2^{f/f}$ and $Grb2^{d/d}$ mice at GD 3.5 (n = 5 per genotype). The results represent the mean ± SEM. ***$p < 0.0001$ by two-tailed unpaired t-test. **f** Immunohistochemistry of stromal maker protein COUP-TFII and **g** Vimentin in the uteri of $Grb2^{f/f}$ and $Grb2^{d/d}$ mice at GD 3.5 (n = 5 per genotype). The results represent the mean ± SEM. *** $p < 0.0001$, and *** $p < 0.0001$ by two-tailed unpaired t-test. Source data are provided in the Source Data file.

near implantation sites of $Grb2^{f/f}$ mice, while they were very weakly detected in luminal epithelium. The levels of stromal pERK1/2 proteins were significantly ($p < 0.001$ and $p < 0.001$, respectively; 3.6-fold and 12.9-fold, respectively) decreased in both Group #1 and Group #2 of $Grb2^{d/d}$ mice compared to control (Fig. 6e, f). These results revealed that GRB2 loss causes dysregulation of ovarian steroid E2/P4 signaling as well as EGFR/ERK signaling in the uterus.

Next, we examined whether tert-Butylhydroquinone (TBHQ), an ERK1/2 activator, rescues the phenotypes of *Grb2* deficient mice. $Grb2^{f/f}$ and $Grb2^{d/d}$ mice were treated daily with TBHQ for 1 week (50 mg/kg via intraperitoneal injection). Unfortunately, TBHQ resulted in implantation failure of control and $Grb2^{d/d}$ mice (Supplementary Fig. 6). Our previous study showed that the expression of ERK1/2 signaling molecules are dynamically regulated during early pregnancy and play a critical role in decidualization[20]. In addition, we examined the effect of U0126, an ERK1/2 inhibitor, during early pregnancy. Control mice were treated with vehicle or U0126 (150 µmol/kg one time/week via intraperitoneal injection) for 1 month and then ultrasound imaging was performed to monitor pregnancy. U0126-treated mice showed a significant decrease ($p = 0.0088$) in the number of implantation sites compared to vehicle group at GD 9.5 (Fig. 7a–c). Therefore, our results suggest that ERK1/2 signaling molecules should be tightly regulated for implantation and decidualization during early pregnancy.

Grb2 is critical for endometrial gland development and function in mouse uterus

Endometrial glands expressing FOXA2 play an important role in the implantation process[6,11,35]. Therefore, we examined gland formation and function in $Grb2^{d/d}$ mice. $Grb2^{d/d}$ mice (8.67 ± 1.67) had significantly fewer endometrial glands compared to controls at GD 3.5 (26.67 ± 2.11, 3.0-fold, $p < 0.001$; Fig. 8a). IHC analysis revealed a significant reduction ($p < 0.001$) of FOXA2, a glandular specific marker, in glands of $Grb2^{d/d}$ mice compared to control mice (Fig. 8b). In order to understand the molecular dysregulation in glands of $Grb2^{d/d}$ mice, we utilized our transcriptomic data from GD 3.5 $Grb2^{d/d}$ mouse uteri to compare the dysregulated genes to those dysregulated in $Pgr^{cre/+}Foxa2^{f/f}$ ($Foxa2^{d/d}$) uteri at GD 3.5[36]. Out of a total of 2,243 genes differentially expressed due to *Grb2* loss, 593 (26.44%) were also differentially expressed in $Foxa2^{d/d}$ mice (Fig. 8c, Supplementary Data 5). Further, a clustering heatmap of the 593 genes identified 343 down-regulated genes in both $Grb2^{d/d}$ and $Foxa2^{d/d}$ mice (Fig. 8d). Importantly, the levels of *Lif* and several glandular epithelium-specific genes (*Prss29*, *Spink3*, *Ttr*, *Wfdc3*) were significantly reduced in the uteri of both $Foxa2^{d/d}$ and $Grb2^{d/d}$ mice compared to controls (Fig. 8e). However, the uterine weight and the expression of FOXA2 were not different ($p = 0.4213$) in the uteri of 3–4-week-old $Grb2^{d/d}$ mice (1.52 ± 0.19) compared to the $Grb2^{f/f}$ mice uteri (1.74 ± 0.16) (n = 4) (Supplementary Fig. 7).

Discussion

Our study reveals that the expression of GRB2 is decreased in eutopic endometrium from infertile women with endometriosis compared to controls. Uterine epithelial-stromal crosstalk is crucial for implantation and decidualization[7]. GRB2 proteins are strongly expressed in uterine epithelial and stromal cells at the pre-implantation stage. However, $Ltf^{icre+}Grb2^{f/f}$ mice revealed normal uterine functions. Interestingly, *GRB2* knock-down in hESC resulted in a significant reduction of decidual markers IGFBP1 and PRL compared to the control (Fig. 4d) and stromal PGR expression was only significantly reduced in $Grb2^{d/d}$ mice compared to control mice (Fig. 5e). Moreover, expression of the stromal markers, vimentin and COUP-TFII, was significantly decreased in the stromal cells of $Grb2^{d/d}$ mice compared to control mice (Fig. 5f, g). Our results suggest that stromal GRB2 plays a critical function for regulation of receptive endometrium and ovarian steroid hormone signaling.

GRB2 binds to EGFR for various biological processes by activating PI3K/AKT and ERK/MAPK pathways[16,17]. Our RNA-seq analysis identified 246 dysregulated EGFR-related genes in the uterus of $Grb2^{d/d}$ mice compared to control. EGFR is critical for endometrial function during early pregnancy[19]. EGFR is expressed in the stroma surrounding the implanting blastocyst[37,38]. However, the expressions of EGFR and pERK1/2 were remarkably decreased in the uterus of $Grb2^{d/d}$ mice at implantation sites of GD 4.5. The defective decidualization responses of eutopic and ectopic endometrial stromal cells in endometriosis patients[39,40] are similar to those observed in $Grb2^{d/d}$ mice as well as hESCs from women without disease with the knock-down of *GRB2*. Importantly, endometrial epithelium-specific *Grb2* knockout mice ($Ltf^{icre/+}Grb2^{f/f}$) exhibited normal implantation and decidualization. Our results suggest that the attenuation of GRB2 in infertile women with endometriosis causes infertility due to implantation failure based on evidence from $Grb2^{d/d}$ mice. However, the molecular mechanism of GRB2 attenuation in the etiology and pathophysiology of endometriosis-related infertility will require further study.

Our previous results showed that mice lacking *Egfr* expression ($Pgr^{cre/+}Egfr^{f/f}$ mice) are severely subfertile[19] as we observed in $Grb2^{d/d}$ mice. Early pregnancy failure and implantation site demise is a key factor in subfertility of both female $Grb2^{d/d}$ and $Pgr^{cre/+}Egfr^{f/f}$ mice. They have the same phenotype that pregnancy demise occurred shortly after blastocyst implantation due to defects in decidualization. Modest reductions in litter size observed in the absence of uterine *Erbb2* or *Erbb3* indicates that they may facilitate EGFR signaling as dimerizing partners but do not play a critical role in pregnancy individually[19]. While *Egf* expression was not changed in $Grb2^{d/d}$ mice, *Erbb2* and *Erbb3* were significantly increased in $Grb2^{d/d}$ mice. These results suggest that *Grb2* targets EGF signaling to regulate uterine function.

$Grb2^{d/d}$ mice exhibited aberrant activation of epithelial proliferation and a decrease in stromal proliferation. Activation of epithelial proliferation at the pre-implantation stage leads to implantation failure in several mutant mouse studies[41,42]. Moreover, the aberrant activation of epithelial proliferation is found in the endometrium of infertile women with endometriosis[43,44]. In contrast, increased stromal cell proliferation is a crucial step for normal uterine receptivity[45] and is considered to be an initiator of decidualization[46]. In the $Grb2^{d/d}$ uterus on GD 4.5, the expression of PTGS2 was significantly reduced in the stromal cells surrounding the embryo at failed implantation sites. This finding suggests that endogenous decidualization was disrupted at the molecular level by loss of GRB2.

The regulation of P4 and E2 is critical for the regulation of the molecular and cellular events leading to the uterine receptivity for

https://doi.org/10.1038/s41467-025-57173-2

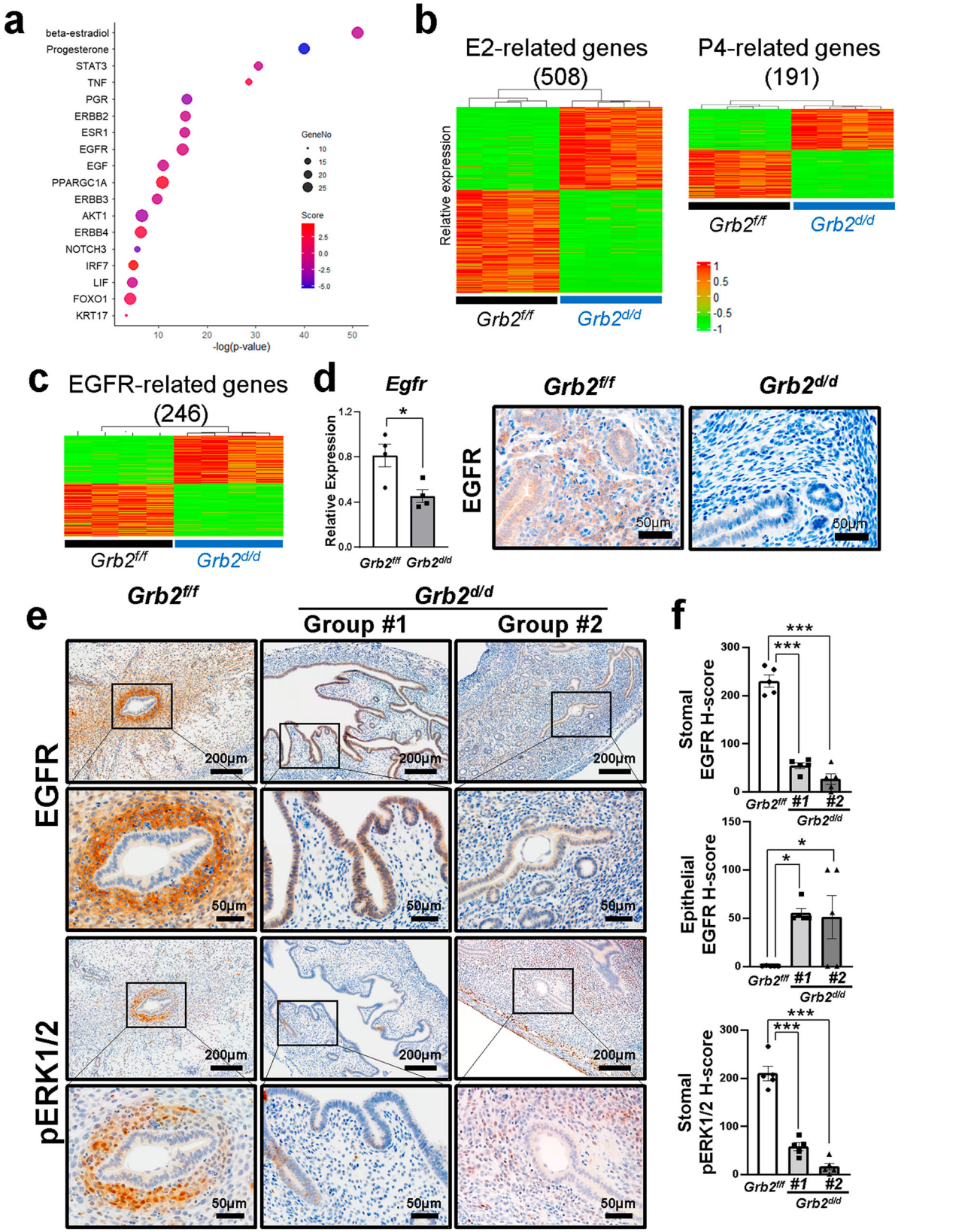

Fig. 6 | Transcriptome profile of the uteri in *Grb2*$^{f/f}$ and *Grb2*$^{d/d}$ mice at GD 3.5. **a** GO terms of the upregulated genes in the uteri of *Grb2*$^{d/d}$ mice compared with that of *Grb2*$^{f/f}$ mice from RNA-seq data. **b** Heatmap of E2-related genes and P4-related genes in the uterus of *Grb2*$^{f/f}$ and *Grb2*$^{d/d}$ mice at GD 3.5. **c** Heatmap of uterine EGFR-related genes and **d** RT-qPCR and immunohistochemistry analysis of EGFR in the uteri of *Grb2*$^{f/f}$ and *Grb2*$^{d/d}$ mice at GD 3.5 (n = 4 per genotype). The results represent the mean ± SEM. *p = 0.0221 by two-tailed unpaired t-test. **e** Immunohistochemistry analysis of EGFR and pERK1/2 in the uteri of *Grb2*$^{f/f}$ and *Grb2*$^{d/d}$ mice at GD 4.5. **f** Semi-quantitative analysis of EGFR and pERK1/2 levels in the uteri of *Grb2*$^{f/f}$ and *Grb2*$^{d/d}$ mice at GD 4.5 (n = 5 per genotype). The results represent the mean ± SEM. ***p < 0.0001, ***p < 0.0001, *p = 0.0300, *p = 0.0455, ***p < 0.0001, and ***p < 0.0001 by Ordinary one-way ANOVA test. Source data are provided in the Source Data file.

https://doi.org/10.1038/s41467-025-57173-2

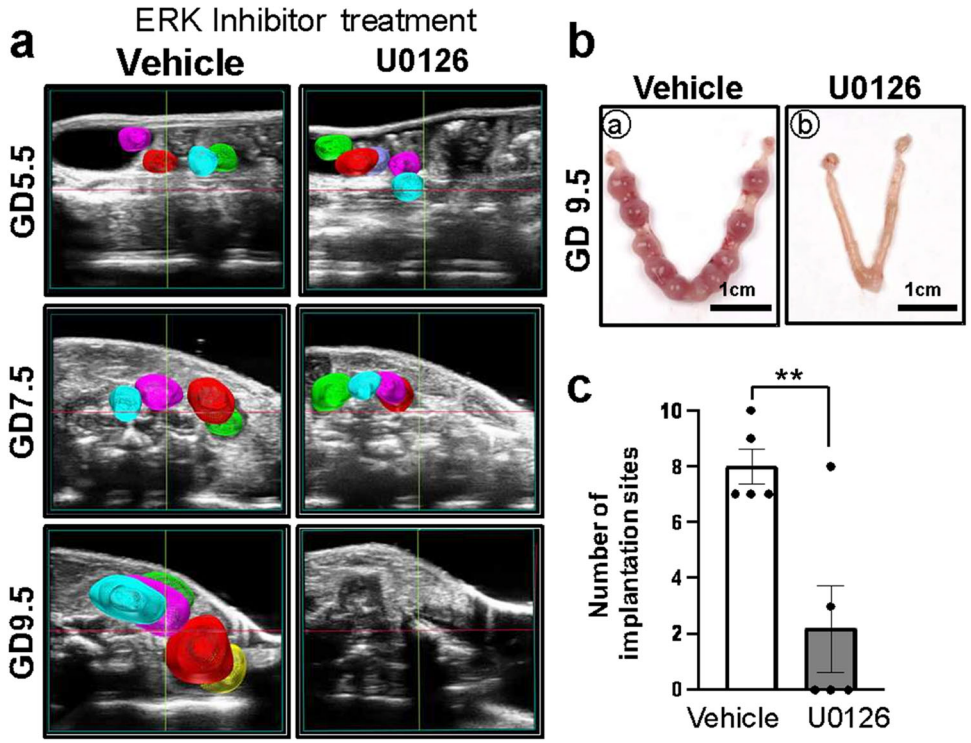

Fig. 7 | ERK signaling is critical for implantation and decidualization. a The number of implantation sites were analyzed by 3D reconstruction of implantations from mice treated with U0126 at GD 5.5, GD 7.5, and GD 9.5 (n = 5 per treatment). **b** Representative image of implantation site of mice treated with vehicle and U0126 at GD 9.5. **c** Mice treated with U0126 shows a decreased number of implantation sites compared with mice treated with vehicle at GD 9.5 (n = 5 per treatment). The results represent the mean ± SEM. $^{**}p = 0.0088$ by two-tailed unpaired t-test. Source data are provided in the Source Data file.

implantation[47]. P4 suppresses E2 action on epithelial proliferation and promotes stromal cell proliferation to prepare uterine receptivity for implantation and decidualization[48]. Loss of E2 action is essential for the implantation at the secretory phase in all eutherian mammal species[43]. The imbalance of P4 and E2 action is found in the endometrium of women with endometriosis[49]. *Grb2*$^{d/d}$ mice revealed dysregulation of PGR and ESR1 in uterine stroma at GD 3.5. As a result, the expression of P4 target genes were significantly reduced, while E2 target genes were significantly upregulated in *Grb2*$^{d/d}$ mice. Failure to downregulate ESR1 signaling is a sign of a homeostasis imbalance in both endometriosis and infertility[50], and is likely the cause of excessive proliferation in the endometrium of women with endometriosis[51].

Interestingly, we found that the number of uterine glands was significantly decreased in the uterus of *Grb2*$^{d/d}$ mice. Uterine glands are critical for implantation and decidualization as reported in uterine *Foxa2*-deleted mice (*Foxa2*$^{d/d}$)[11,35]. FOXA2 is explicitly expressed in the glandular epithelium of uterus in both mice and human[52,53]. FOXA2 was decreased in eutopic endometrium from women with endometriosis[54]. In *Foxa2*$^{d/d}$ mice, the absence of uterine glands led to severe defects of implantation and decidualization[35,53]. We observed that the expression of FOXA2 was significantly decreased in the glandular epithelium in the uterus of *Grb2*$^{d/d}$ mice. *Grb2*$^{d/d}$ and both FOXA2-deficient mouse models (*Foxa2*$^{d/d}$ and *Ltf*$^{icre/+}$*Foxa2*$^{f/f}$) are infertile due to defects in embryo attachment on GD 4.5[11,35]. Furthermore, our comparative analysis of transcriptomic data from *Grb2*$^{d/d}$ and *Foxa2*$^{d/d}$ mice confirmed the molecular impact of uterine *Grb2* loss on FOXA2-regulated genes.

In conclusion, our findings demonstrate that GRB2 plays a critical role for the successful progression of early pregnancy. As we observed attenuation of GRB2 in human eutopic endometrium from infertile women with endometriosis, loss of *Grb2* in the mouse uterus resulted in infertility due to implantation and decidualization defects. Interestingly, the ablation of *Grb2* in the uterus impaired uterine gland function normally supported by FOXA2. Therefore, our studies suggest a conceptual framework for understanding abnormal endometrial homeostasis, with implications for the diagnosis and treatment of a non-receptive endometrium in early pregnancy loss.

Methods

Study design

The main objective of this study was to evaluate the role of GRB2 in infertility. First, the expression of GRB2 was assessed in eutopic endometrium of infertile women with or without endometriosis compared to fertile women. To determine whether endometriosis affects GRB2 expression, GRB2 protein expression were examined in a mouse model of endometriosis. Subsequently, we determine that impact of *Grb2* ablation on the infertility implantation, and decidualization in *Grb2*$^{d/d}$ and littermate control mice. Finally, transcriptomic analysis was applied to dissect the molecular mechanisms of *Grb2* in the uterus. The control and treatment groups and the number of biological replicates (sample sizes) for each experiment are specified in the figure legends. The number of animals for each study type were determined by the investigators on the basis of previous experience with the standard disease models that were used or from pilot studies. Animals were randomly allocated to the control and treatment groups and housed together to minimize environmental differences and experimental bias. Analysis of endpoint readouts was carried out in a blinded fashion.

Ethics statement and declarations

The institutional review boards of University of Missouri, Wake Forest University, and University of North Carolina approved this study. The Institutional Animal Care and Use Committee at University of Missouri approved all experiments relating to mice.

All animal experiments were approved by the University of Missouri Animal Care and Use Committee. Mice were housed and bred in a

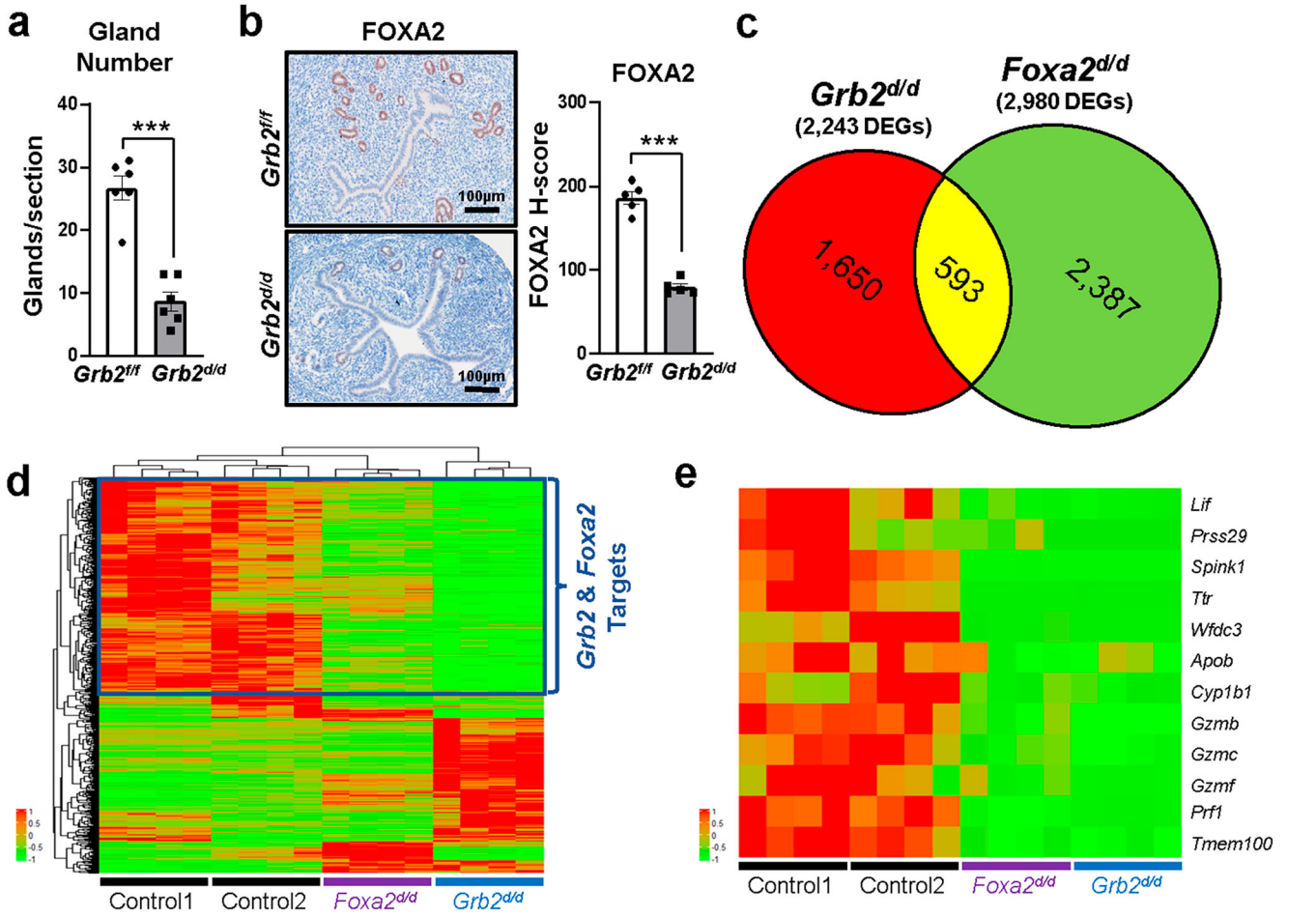

Fig. 8 | A decrease of FOXA2 expression in the uteri in *Grb2*$^{d/d}$ mice at GD 3.5. **a** The number of grands in the uteri of *Grb2*$^{f/f}$ and *Grb2*$^{d/d}$ mice at GD 3.5 (n = 6). The results represent the mean ± SEM. ***$p < 0.0001$ by two-tailed unpaired t-test. **b** Immunohistochemistry analysis of FOXA2 in the uteri of *Grb2*$^{f/f}$ and *Grb2*$^{d/d}$ mice at GD 3.5 (n = 5 per treatment). The results represent the mean ± SEM. ***$p < 0.0001$ by two-tailed unpaired t-test. **c** Venn diagram of identifying genes that overlapped in RNA-Seq data between *Foxa2*$^{d/d}$ and *Grb2*$^{d/d}$ mice at GD 3.5. **d** A heatmap of differentially expressed genes in uterus of control, *Foxa2*$^{d/d}$ and *Grb2*$^{d/d}$ mice at GD 3.5 from RNA-Seq data (n = 4 per genotype). **e** Heatmap of *Grb2* and *Foxa2*-related genes in the uteri of *Foxa2*$^{d/d}$ and *Grb2*$^{d/d}$ mice at GD 3.5 (n = 4 per genotype). Source data are provided in the Source Data file.

designated animal care facility at University of Missouri with controlled humidity and temperature conditions and a 12 h light/dark cycle.

Human endometrium samples

The human endometrial samples used to examine GRB2 expression patterns were obtained from Wake Forest University and University of North Carolina. Written informed consent was obtained from all participants. The study design and conduct complied with all relevant regulations regarding the use of human study participants and was conducted in accordance with the criteria set by the Declaration of Helsinki. Control endometrial tissues were laparoscopically negative for endometriosis and had not been on any hormonal therapies for at least 3 months prior to surgery. Histologic dating of endometrial samples was done on the basis of the criteria of Noyes et al.[55] and confirmed by subsequent histopathological examination by an experienced fertility specialist (B.A.L.). Normally cycling women without infertility who were free of hormones for at least 60 days served as fertile controls. Tubal ligation was a source for normal subjects as it allows us to rule out endometriosis laparoscopically. All endometriosis-related infertility cases were undergoing endometrial sampling prior to surgical removal of endometriosis. All patients did not have uterine leiomyoma and adenomyosis. To investigate GRB2 amounts in the endometrium from women, 18 infertile women with endometriosis, 13 infertile women without endometriosis and 19 control eutopic endometrium were used. Samples used for immunohistochemistry were fixed in 10% buffered formalin prior to embedding in paraffin wax.

Animals and tissue collection

Mice were housed and bred in a designated animal care facility at the University of Missouri with controlled humidity (30-70%) and temperature conditions (68–79 °F) and a 12 h light/dark cycle. *Grb2* conditional knockout mice were generated crossing *Pgr*$^{cre/+22}$ or *Ltf*$^{icre/+56}$ males with female mice carrying the *Grb2*$^{f/f}$ allele (*Pgr*$^{cre/+}$*Grb2*$^{f/f}$; *Grb2*$^{d/d}$). All control (*Grb2*$^{f/f}$), *Pgr*$^{cre/+}$*Grb2*$^{f/f}$, and *Ltf*$^{icre/+}$ *Grb2*$^{f/f}$ mice were mixed background C57BL/6J and 129S1/SvImJ strains and 8-12-week-old female mice from. were used for all experiments. For the early pregnancy study, female *Grb2*$^{f/f}$ and *Grb2*$^{d/d}$ were mated with C57BL/6 male mice, and uterine samples from pregnant mice were obtained at different days of pregnancy. The morning of vaginal plug is designated as GD 0.5. Uteri were collected at GD 3.5 and 4.5, and implantation sites were visualized on GD 4.5 by intravenous injection of 1% Chicago Sky Blue 6B dye (Sigma-Aldrich, St. Louis, MO). Fertility was assessed by mating female *Grb2*$^{f/f}$ and *Grb2*$^{d/d}$ mice with wild-type C57BL/6 male mice for 6 months. The number of litter and pups born during that period was recorded. U0126 was purchased from Selleck (Pennsylvania, USA) and tert-Butylhydroquinone (TBHQ) was purchased from MedChemExpress (New Jersey, USA). For ERK inhibitor and activator

study, U0126 and TBHQ were dissolved in solution 5% DMSO + 40% PEG400 + 45% Saline + 5% Tween80. For U0126 treatment study, female control mice at 8 weeks old were received with either vehicle (PBS) and U0126 (150 μmol/kg) every week by intraperitoneal (i.p) injection for 2 weeks. For TBHQ treatment study, *Grb2*$^{f/f}$ and *Grb2*$^{d/d}$ mice were daily received with TBHQ (50 mg/kg) by intraperitoneal (i.p) injection for 1 week. After the last injection, mice were mated with wild-type male mice. Vevo F2 LAZR-X ultrasound system was used at GD 5.5, 7.5, and 9.5. Uterine tissues were collected at the time of dissection and immediately either fixed with 4% (vol/vol) paraformaldehyde for histology or immunohistochemistry or snap frozen and stored at −80 °C for RNA/protein extraction. The levels of progesterone and estrogen in serum were measured by the University of Virginia Center for Research in Reproduction Ligand Assay and Analysis Core.

Induction of endometriosis in mouse

The endometriosis was induced in 8-week-old female control (*Pgr*$^{cre/+}$*Rosa26*^{mTmG}) and *Grb2*$^{d/d}$ *Rosa26*^{mTmG} mice which have conditional double-fluorescent Cre reporter gene had daily 1 μg/ml of E2 injection for 3 days and then autologous endometriosis induction were performed[57]. After 1 month post endometriosis induction, the mice were euthanized, and endometriotic lesions were counted under fluorescence microscope.

Reverse transcription-quantitative PCR

1 μg of RNA was used for reverse transcription with MMLV Reverse Transcriptase (Invitrogen, Carlsbad, CA) according to the manufacturer's instructions. mRNA expression levels of genes of interest were measured by real-time PCR TaqMan or SYBR green analysis using an Applied Biosystems StepOnePlus system (Applied Biosystems, Foster City, CA, USA). The mRNA quantities were normalized against the housekeeping gene, 60S ribosomal protein L7. Analysis of mRNA expression was first undertaken by the standard curve method, and results were corroborated by cycle threshold values assessing gene expression. Primer sequences used in these studies are shown in Supplementary Table 1.

Histology and immunostaining

Histology and immunohistochemistry analyses were performed as previously described[54,58].

For immunohistochemistry, dewaxed hydrated paraffin-embedded tissue sections were blocked with 10% normal goat serum in PBS (pH 7.5) and then incubated with primary antibody diluted in 10% normal goat serum in PBS (pH 7.5) overnight at 4 °C anti-GRB2 (1:2000 dilution; ab32037; Abcam), anti-PTGS2 (1:500 dilution; 160106; Cayman), anti-FOXO1 (1:500 dilution; CS-2880; Cell Signaling), anti-PGR (1:2000 dilution; CS-8757S; Cell Signaling), anti-EGFR (1:500 dilution; CS-2646; Cell Signaling), anti-ERBB2 (1:1000 dilution; CS-4290S; Cell Signaling), anti-pERK (1:500 dilution; CS-4370; Cell Signaling), anti-COUP-TFII (1:1000 dilution; PP-H7147-10; Perseus Proteomics), anti-Vimentin (1:1000 dilution; ab92547; Abcam), anti-FOXA2 (1:1000 dilution; WRAB-FOXA2; Seven Hills BioReagent), anti-Ki67 (1:1000 dilution; BD550609; BD Pharmingen), anti-ERα (1:1000 dilution; sc-8002; Santa Cruz). On the next day, the sections were incubated with the appropriate species specific HRP-conjugated secondary antibody (2 μg/ml; Vector Laboratories) for 1 h at room temperature. Immunoreactivity was detected using the Vectastain Elite DAB kit (Vector Laboratories). A semi-quantitative grading system (H-score) was used to compare the immunohistochemical staining intensities as previously described[59]. The overall score ranged from 0 to 300.

Western blot analysis

Proteins were extracted using lysis buffer (10 mM Tris-HCl (pH 7.4), 150 mM NaCl, 2.5 mM EDTA, and 0.125% Nonidet P-40 (vol/vol)) supplemented with both a protease inhibitor cocktail (Roche, Indianapolis, IN) and a phosphatase inhibitor cocktail (Sigma-Aldrich, St. Louis, MO). Ten micrograms of total protein was electrophoresed via 8% SDS–PAGE gels and transferred into a polyvinylidene difluoride membrane (Millipore Corp., Bedford, MA, USA). Membrane was blocked with Casein (0.5% w/v) in PBS with 0.1% Tween 20 (v/v; Sigma-Aldrich) prior to exposure to anti-GRB2 (1:20,000 dilution; CS-3972; Cell Signaling) antibody. Total β-Actin (1:20,000 dilution; SAB5600204; Sigma) levels were examined for loading controls. Immunoreactivity was visualized by incubation with a horseradish peroxidase-linked secondary antibody (anti-Rabit IgG (1:5000 dilution; PI-9500; Vector Laboratories)) followed by exposure to Electrochemiluminescence reagents (ECL) according to the manufacturer's instructions (GE Healthcare Biosciences).

Ultrasound imaging

To examine the size of embryo during the early pregnancy, the Vevo F2 LAZR-X small animal ultrasound system (FUJIFILM VisualSonics Inc., Toronto, Canada), a non-invasion high resolution imaging tool, was used at GD 5.5, 7.5 and 9.5. Mice were anesthetized using isoflurane and positioned supine on a heated imaging stage with the face toward the scientist. ECG, body temperature, and respiratory physiology were always controlled. Eye creme was put on mice's eyes to protect and maintain the physiological ocular welfare. The hair on the abdomen was removed with commercial hair removal cream. Then pre-warmed ultrasound gel was applied directly onto the depilated skin. First, the transducer 47 MHz (MS550D-0421) was used to identify the bladder as reference point. B-Mode or brightness mode was used to render a two-dimensional gray scale image of anatomical structures. A motor was attached to the transducer to translate the transducer from the left to the right side of the abdomen with step sizes of scanning (10 μm). The acquired 2D images were processed with Vevo Lab software (Fujifilm, VisualSonics, version 5.5.1) to reconstruct and analysis the 3D volume of implantations to obtain transverse, sagittal, and coronal representations of implantations.

Artificial decidualization response

To test the uterine response to an artificial decidual stimulus, female *Grb2*$^{f/f}$ and *Grb2*$^{d/d}$ mice were ovariectomized at 6 weeks of age, allowed to recover for 2 weeks as described previously study[60]. Then mice were subjected to the following hormonal regimen: 100 ng of E2 per day for 3 days; 2 days rest; then three daily injections of 1 mg of P4 plus 6.7 ng of E2. To induce artificial decidualization, the left uterine horn was mechanically stimulated by scratching the full length of the anti-mesometrial side with a burred needle 6 h following the third P4 and E2 injection. The other horn was left unstimulated as a control. Daily injections of P4 (1 mg/mouse) + E2 (6.7 ng/mouse) were continued for 5 days to maximize the decidual response. Then, mice were sacrificed on day 5. The uteri were then excised, weighed, and fixed in 4% paraformaldehyde for histological analysis. For RNA or protein extractions, uterine tissues were collected and immediately frozen in dry ice.

hESC culture and in vitro decidualization

Human primary endometrial stromal cells (hESCs) were isolated from pure endometrial tissue by collagenase digestion[20,61,62]. Briefly, endometrial tissue was minced and digested twice at 37 °C in buffered saline supplemented with 0.5% collagenase (Sigma-Aldrich, St. Louis, MO) and 0.002% DNase (Sigma-Aldrich, St. Louis, MO). Then endometrial tissues were filtered through 70 μm sterile sieves to exclude epithelium. The remaining hESCs were cultured at 37 °C in 5% CO2, and incubated with RPMI-1640 phenol red–free medium (Gibco, Grand Island, NY) contained 0.1 mM sodium pyruvate (Gibco, Grand Island, NY), 10% fetal bovine serum (FBS; Gibco, Grand Island, NY), and 1% penicillin streptomycin (P/S; Gibco, Grand Island, NY). Small interfering RNA (siRNA) of GRB2 (L-019220-00-0020, Dharmacon, Lafayette,

CO) was used for the knock-down of GRB2 gene expression and non-targeting scrambled siRNA (NC1486135, Dharmacon) was used as a control. Transfection of hESC were conducted using lipofectamine 2000 (Invitrogen, Carlsbad, CA) based on the manufacturer's instructions. In brief, after 4 h of serum starvation, hESCs were incubated in serum-free media with transfection complex for 6 h before replacing with growth media and incubating for 2 days before in vitro decidualization induction. To induce in vitro decidualization, hESC were incubated with differentiation media contained OPTI-MEM medium (Gibco) with 2% FBS depleted of steroids by pretreatment with dextran-coated charcoal (CSFBS; Gibco), 10 nM 17β-estradiol (E2; Sigma-Aldrich, St. Louis, MO), 1 μM medroxyprogesterone acetate (Sigma-Aldrich), 50 μM Cyclic adenosine monophosphate (cAMP; Sigma-Aldrich), and 1% Penicillin and streptomycin (P/S; Gibco). Differentiation media were replaced every 2 days until the 6 days.

RNA-sequencing analysis

Total RNA was extracted from the uterine tissues using the RNeasy total RNA isolation kit (Qiagen, Valencia, CA). NanoDrop was used to determine RNA purity and for an initial estimate of RNA concentration. For RNA-Seq, 500 ng of total RNA were used. RNA-Seq libraries were prepared by the Van Andel Genomics Core using the KAPA mRNA Hyperprep kit (v4.17) (Kapa Biosystems, Wilmington, MA, USA). RNA was sheared to 300–400 bp. Prior to PCR amplification, cDNA fragments were ligated to IDT for Illumina unique dual adapters (IDT DNA Inc). Quality and quantity of libraries were assessed using a combination of Agilent DNA High Sensitivity chip (Agilent Technologies, Inc.) and QuantiFluor® dsDNA System (Promega Corp., Madison, WI, USA). Individually indexed libraries were pooled and 50 bp, paired end sequencing was performed using an Illumina NovaSeq6000 sequencer and S2, 100 cycle sequencing kit (Illumina Inc., San Diego, CA, USA). Each library was sequenced to an average raw depth of 50 M reads. Base calling was done by Illumina RTA3 and output of NCS was demultiplexed and converted to FastQ format with Illumina Bcl2fastq v1.9.0. The raw reads were initially filtered by removing low quality reads (average quality scores <20) and aligned to the mm39 genome using Star 2.7.9a[63]. The differentiated expressions of genes (DEGs) were determined by the exact test of EdgeR[64]. The DEGs were determined as maximum counts ≥1; fold change of >2 (upregulated) or <−2 (down-regulated), FDR < 0.05. The Principle Component Analysis (PCA) map were generated by plotMDS in EdgeR[64]. The expressions of DEGs were normalized, scaled, clustered to generate the heatmap using the ComplexHeatmap package[65]. The significantly enriched pathways and upstream regulators based on the DEGs were identified using Ingenuity pathway analysis (IPA, Qiagen). The dotplot was generated by Tidyverse package[66].

Comparative transcriptomic analysis

Comparisons of GD 3.5 *Grb2*$^{d/d}$ to GD 3.5 *Foxa2*$^{d/d}$ uterine dysregulated genes were performed by comparing differentially expressed genes determined between differentially expressed genes of *Grb2*$^{d/d}$ mice with differentially expressed genes determined by previously reported transcriptomics analysis of *Foxa2*$^{d/d}$ mice publicly available from the GEO database (GSE48339)[36]. The differentially expressed gene lists of *Foxa2*$^{d/d}$ mice used for comparative transcriptomics were prepared by original authors of the studies according to their published methods of analysis[36]. Duplicate genes present in the gene lists (due to the presence of multiple array probes for some genes) were removed based on GeneBank ID or gene symbol. Briefly, the transcriptome of *Grb2*$^{d/d}$ at GD 3.5 overlapped with *Foxa2*$^{d/d}$ transcriptome at GD 3.5.

Statistical analysis

To assess statistical significance of parametric data, the Student's t-test was used for data with only two groups. For data containing more than two groups, one-way ANOVA was used, followed by Tukey's post hoc test for multiple comparisons. All data are presented as means ± SEM. $p < 0.05$ was considered statistically significant. All statistical analyses were performed using the Instat package from GraphPad (San Diego, CA, USA).

Reporting summary

Further information on research design is available in the Nature Portfolio Reporting Summary linked to this article.

Data availability

The RNA-seq data generated in this study have been deposited in the NCBI Gene Expression Omnibus database under accession code GSE260505 and previously reported transcriptomics analysis of *Foxa2*$^{d/d}$ mice is publicly available under accession code GSE48339[36]. The all data generated in this study are provided in the Supplementary Information/Source Data file. Source data are provided with this paper.

References

1. Messaoudi, S. et al. 15 years of transcriptomic analysis on endometrial receptivity: what have we learnt? *Fertil. Res. Pr.* **5**, 9 (2019).
2. Cha, J., Sun, X. & Dey, S. K. Mechanisms of implantation: strategies for successful pregnancy. *Nat. Med.* **18**, 1754–1767 (2012).
3. Patel, B. et al. Role of nuclear progesterone receptor isoforms in uterine pathophysiology. *Hum. Reprod. Update* **21**, 155–173 (2015).
4. Stewart, C. L. et al. Blastocyst implantation depends on maternal expression of leukaemia inhibitory factor. *Nature* **359**, 76–79 (1992).
5. Kelleher, A. M., DeMayo, F. J. & Spencer, T. E. Uterine glands: developmental biology and functional roles in pregnancy. *Endocr. Rev.* **40**, 1424–1445 (2019).
6. Kelleher, A. M., Milano-Foster, J., Behura, S. K. & Spencer, T. E. Uterine glands coordinate on-time embryo implantation and impact endometrial decidualization for pregnancy success. *Nat. Commun.* **9**, 2435 (2018).
7. Hantak, A. M., Bagchi, I. C. & Bagchi, M. K. Role of uterine stromal-epithelial crosstalk in embryo implantation. *Int. J. Dev. Biol.* **58**, 139 (2014).
8. Spencer T. E. Biological roles of uterine glands in pregnancy. *Semin. Reprod. Med.* **32**, 346–357 (2014).
9. Yuan, J. et al. Tridimensional visualization reveals direct communication between the embryo and glands critical for implantation. *Nat. Commun.* **9**, 603 (2018).
10. Burton, G., Jauniaux, E. & Charnock-Jones, D. Human early placental development: potential roles of the endometrial glands. *Placenta* **28**, S64–S69 (2007).
11. Jeong, J.-W. et al. Foxa2 is essential for mouse endometrial gland development and fertility. *Biol. Reprod.* **83**, 396–403 (2010).
12. Besnard, V., Wert, S. E., Hull, W. M. & Whitsett, J. A. Immunohistochemical localization of Foxa1 and Foxa2 in mouse embryos and adult tissues. *Gene Expr. Patterns* **5**, 193–208 (2004).
13. Dhakal, P., Fitzgerald, H. C., Kelleher, A. M., Liu, H. & Spencer, T. E. Uterine glands impact embryo survival and stromal cell decidualization in mice. *FASEB J.* **35**, e21938 (2021).
14. Wee, P. & Wang, Z. Epidermal growth factor receptor cell proliferation signaling pathways. *Cancers* **9**, 52 (2017).
15. Lim, S.-J., Lopez-Berestein, G., Hung, M.-C., Lupu, R. & Tari, A. M. Grb2 downregulation leads to Akt inactivation in heregulin-stimulated and ErbB2-overexpressing breast cancer cells. *Oncogene* **19**, 6271–6276 (2000).
16. Ijaz, M. et al. The role of Grb2 in cancer and peptides as Grb2 antagonists. *Protein Pept. Lett.* **24**, 1084–1095 (2017).
17. Sattler, M. et al. Critical role for Gab2 in transformation by BCR/ABL. *Cancer Cell* **1**, 479–492 (2002).
18. Modi, H. et al. Inhibition of Grb2 expression demonstrates an important role in BCR–ABL-mediated MAPK activation and

transformation of primary human hematopoietic cells. *Leukemia* **25**, 305–312 (2011).
19. Large, M. J. et al. The epidermal growth factor receptor critically regulates endometrial function during early pregnancy. *PLoS Genet.* **10**, e1004451 (2014).
20. Lee, C. H. et al. Extracellular signal-regulated kinase 1/2 signaling pathway is required for endometrial decidualization in mice and human. *PLoS ONE* **8**, e75282 (2013).
21. Krehbiel, R. H. Cytological studies of the decidual reaction in the rat during early pregnancy and in the production of deciduomata. *Physiological Zool.* **10**, 212–234 (1937).
22. Soyal, S. M. et al. Cre-mediated recombination in cell lineages that express the progesterone receptor. *Genesis* **41**, 58–66 (2005).
23. Sun, X. et al. Kruppel-like factor 5 (KLF5) is critical for conferring uterine receptivity to implantation. *Proc. Natl. Acad. Sci. USA* **109**, 1145–1150 (2012).
24. Vasquez, Y. M. et al. FOXO1 regulates uterine epithelial integrity and progesterone receptor expression critical for embryo implantation. *PLoS Genet.* **14**, e1007787 (2018).
25. Takano, M. et al. Transcriptional cross talk between the forkhead transcription factor forkhead box O1A and the progesterone receptor coordinates cell cycle regulation and differentiation in human endometrial stromal cells. *Mol. Endocrinol.* **21**, 2334–2349 (2007).
26. Wetendorf, M. & DeMayo, F. J. The progesterone receptor regulates implantation, decidualization, and glandular development via a complex paracrine signaling network. *Mol. Cell. Endocrinol.* **357**, 108–118 (2012).
27. Klemmt, P. A., Carver, J. G., Kennedy, S. H., Koninckx, P. R. & Mardon, H. J. Stromal cells from endometriotic lesions and endometrium from women with endometriosis have reduced decidualization capacity. *Fertil. Steril.* **85**, 564–572 (2006).
28. Kim, J. J., Jaffe, R. C. & Fazleabas, A. T. Comparative studies on the in vitro decidualization process in the baboon (Papio anubis) and human. *Biol. Reprod.* **59**, 160–168 (1998).
29. Liang, X. et al. The uterine epithelial loss of Pten is inefficient to induce endometrial cancer with intact stromal Pten. *PLoS Genet.* **14**, e1007630 (2018).
30. Tan, J., Paria, B. C., Dey, S. K. & Das, S. K. Differential uterine expression of estrogen and progesterone receptors correlates with uterine preparation for implantation and decidualization in the mouse. *Endocrinology* **140**, 5310–5321 (1999).
31. Brenner, R. M., West, N. B. & McClellan, M. C. Estrogen and progestin receptors in the reproductive tract of male and female primates. *Biol. Reprod.* **42**, 11–19 (1990).
32. Lessey, B. A. et al. Immunohistochemical analysis of human uterine estrogen and progesterone receptors throughout the menstrual cycle. *J. Clin. Endocrinol. Metab.* **67**, 334–340 (1988).
33. Yoshinaga, K. Uterine receptivity for blastocyst implantation. *Ann. N. Y. Acad. Sci.* **541**, 424–431 (1988).
34. Young, S. L. & Lessey, B. A. Progesterone function in human endometrium: clinical perspectives. *Semin. Reprod. Med.* **28**, 5–16 (2010).
35. Kelleher, A. M. et al. Forkhead box a2 (FOXA2) is essential for uterine function and fertility. *Proc. Natl. Acad. Sci. USA* **114**, E1018–E1026 (2017).
36. Filant, J., Lydon, J. P. & Spencer, T. E. Integrated chromatin immunoprecipitation sequencing and microarray analysis identifies FOXA2 target genes in the glands of the mouse uterus. *FASEB J.* **28**, 230–243 (2014).
37. Das, S., Tsukamura, H., Paria, B., Andrews, G. & Dey, S. Differential expression of epidermal growth factor receptor (EGF-R) gene and regulation of EGF-R bioactivity by progesterone and estrogen in the adult mouse uterus. *Endocrinology* **134**, 971–981 (1994).
38. Tong, B. J., Das, S., Threadgill, D., Magnuson, T. & Dey, S. Differential expression of the full-length and truncated forms of the epidermal growth factor receptor in the preimplantation mouse uterus and blastocyst. *Endocrinology* **137**, 1492–1496 (1996).
39. Bui, A. H., Timmons, D. B. & Young, S. L. Evaluation of endometrial receptivity and implantation failure. *Curr. Opin. Obstet. Gynecol.* **34**, 107–113 (2022).
40. Lessey, B. A. & Young, S. L. What exactly is endometrial receptivity? *Fertil. Steril.* **111**, 611–617 (2019).
41. Kim, T. H. et al. ARID1A is essential for endometrial function during early pregnancy. *PLoS Genet.* **11**, e1005537 (2015).
42. Kim, T. H. et al. Role of SIRT1 and progesterone resistance in normal and abnormal endometrium. *J. Clin. Endocrinol. Metab.* **107**, 788–800 (2022).
43. Fox, C., Morin, S., Jeong, J.-W., Scott, R. T. Jr & Lessey, B. A. Local and systemic factors and implantation: what is the evidence? *Fertil. Steril.* **105**, 873–884 (2016).
44. Lessey, B. A. & Kim, J. J. Endometrial receptivity in the eutopic endometrium of women with endometriosis: it is affected, and let me show you why. *Fertil. Steril.* **108**, 19–27 (2017).
45. Daikoku, T. et al. Conditional deletion of Msx homeobox genes in the uterus inhibits blastocyst implantation by altering uterine receptivity. *Dev. Cell* **21**, 1014–1025 (2011).
46. Das, S. K. Regional development of uterine decidualization: molecular signaling by Hoxa-10. *Mol. Reprod. Dev. Incorp. Gamete Res.* **77**, 387–396 (2010).
47. Dey, S. et al. Molecular cues to implantation. *Endocr. Rev.* **25**, 341–373 (2004).
48. Li, Q. et al. The antiproliferative action of progesterone in uterine epithelium is mediated by Hand2. *Science* **331**, 912–916 (2011).
49. Lessey B. A. & Young S. L. Homeostasis imbalance in the endometrium of women with implantation defects: the role of estrogen and progesterone. *Semin. Reprod. Med.* **32**, 365–375 (2014).
50. Lessey, B. A., Palomino, W. A., Apparao, K. B., Young, S. L. & Lininger, R. A. Estrogen receptor-alpha (ER-alpha) and defects in uterine receptivity in women. *Reprod. Biol. Endocrinol.* **4**(Suppl 1), S9 (2006).
51. Park, J. S. et al. Endometrium from women with endometriosis shows increased proliferation activity. *Fertil. Steril.* **92**, 1246–1249 (2009).
52. Villacorte, M. et al. β-Catenin signaling regulates Foxa2 expression during endometrial hyperplasia formation. *Oncogene* **32**, 3477–3482 (2013).
53. Filant, J. & Spencer, T. E. Endometrial glands are essential for blastocyst implantation and decidualization in the mouse uterus. *Biol. Reprod.* **88**, 93 (2013).
54. Marquardt, R. M. et al. Endometrial epithelial ARID1A is critical for uterine gland function in early pregnancy establishment. *FASEB J.* **35**, e21209 (2021).
55. Noyes, R. W., Hertig, A. T. & Rock, J. Dating the endometrial biopsy. *Am. J. Obstet. Gynecol.* **122**, 262–263 (1975).
56. Daikoku, T. et al. Lactoferrin-iCre: a new mouse line to study uterine epithelial gene function. *Endocrinology* **155**, 2718–2724 (2014).
57. Yoo, J.-Y. et al. Loss of MIG-6 results in endometrial progesterone resistance via ERBB2. *Nat. Commun.* **13**, 1101 (2022).
58. Kim, B. G. et al. Aberrant activation of signal transducer and activator of transcription-3 (STAT3) signaling in endometriosis. *Hum. Reprod.* **30**, 1069–1078 (2015).
59. Ishibashi, H. et al. Sex steroid hormone receptors in human thymoma. *J. Clin. Endocrinol. Metab.* **88**, 2309–2317 (2003).
60. Finn, C. & Martin, L. Endocrine control of the timing of endometrial sensitivity to a decidual stimulus. *Biol. Reprod.* **7**, 82–86 (1972).

61. Yoo, J.-Y. et al. G-protein coupled receptor 64 is required for decidualization of endometrial stromal cells. *Sci. Rep.* **7**, 5021 (2017).
62. Kim, T. H. et al. Loss of HDAC3 results in nonreceptive endometrium and female infertility. *Sci. Transl. Med.* **11**, eaaf7533 (2019).
63. Dobin, A. et al. STAR: ultrafast universal RNA-seq aligner. *Bioinformatics* **29**, 15–21 (2013).
64. Robinson, M. D., McCarthy, D. J. & Smyth, G. K. edgeR: a Bioconductor package for differential expression analysis of digital gene expression data. *Bioinformatics* **26**, 139–140 (2010).
65. Gu, Z. G., Eils, R. & Schlesner, M. Complex heatmaps reveal patterns and correlations in multidimensional genomic data. *Bioinformatics* **32**, 2847–2849 (2016).
66. Wickham, H. et al. Welcome to the tidyverse. *J. Open Source Softw.* **4**, 1686 (2019).

Acknowledgements

This work was supported by the Eunice Kennedy Shriver National Institute of Child Health & Human Development of the National Institutes of Health under Award Numbers R01HD102170 and R01HD101243 (to J.W.J.) and the National Reserch Foundation of Korea founded by Korea Government under Award Number RS-2023-NR077285 (to Y.P.C). The content is solely the responsibility of the authors and does not necessarily represent the official views of the National Institutes of Health.

Author contributions

Y.P.C. and J.W.J. were responsible for the concept of the study; S.L.Y. and B.A.L. collected human samples; D.N.T., Y.J.H., K.C.K., and T.H.K. carried out experiments; R.M.M., R.L., T.H.K. and J.W.J. analyzed data; C.C. provided transgenic mice; D.N.T., R.M.M., T.H.K., Y.P.C., and J.W.J. contributed to writing the manuscript. All authors contributed to the final manuscript version.

Competing interests

The authors declare no competing interests.

Additional information

Supplementary information The online version contains supplementary material available at https://doi.org/10.1038/s41467-025-57173-2.

Correspondence and requests for materials should be addressed to Yong-Pil Cheon or Jae-Wook Jeong.

Peer review information *Nature Communications* thanks the anonymous reviewer(s) for their contribution to the peer review of this work. A peer review file is available.